

Determination of accumulation rates from a shallow firn core of the West Antarctic Ice Sheet

Master's Thesis

Faculty of Science

University of Bern

presented by

Jacqueline Fenwick

2014

Supervisor:

Prof. Dr Margit Schwikowski

Paul Scherrer Institut and Oeschger Centre for Climate Change Research

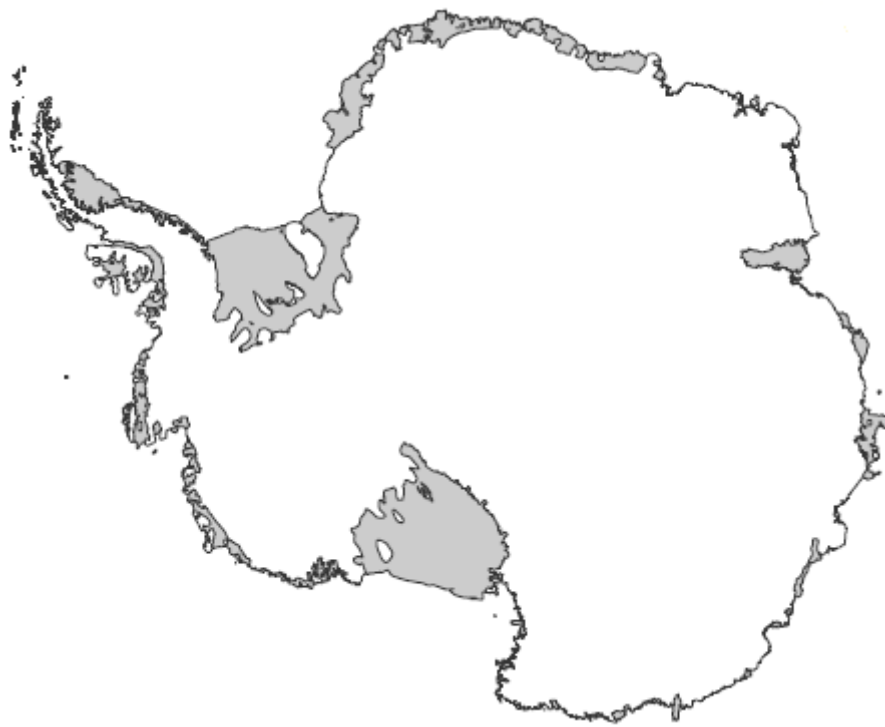
Co-Supervisor:

Dr Anja Eichler

Paul Scherrer Institut

West Side Story: Determination of accumulation rates from a shallow firn core of the West Antarctic Ice Sheet

Jacqueline Fenwick



u^b

UNIVERSITÄT
BERN

OESCHGER CENTRE
CLIMATE CHANGE RESEARCH

PAUL SCHERRER INSTITUT



Abstract

In recent decades the West Antarctic Ice Sheet has experienced warming and glacial retreat. Despite receiving growing attention, knowledge of glacial dynamics in this region remains limited. Snow accumulation data is sparse and fails to capture true spatial variability. A shallow firn core, drilled at the triple ice divide between Pine Island Glacier, Institute Ice Stream, and Rutford Ice Stream, was glaciochemically analysed. Oxygen and hydrogen stable isotopes measured using Cavity Ringdown Spectroscopy exhibited seasonal oscillations. Ion concentrations measured with Ion Chromatography likewise varied seasonally, with maximum sodium, chloride and potassium concentrations in winter and maximum methanesulfonate, sulphate and nitrate concentrations in summer. Despite melt damage to the core during transport, it was possible to determine 18 annual layers and calculate an average accumulation rate of around 25 cm water equivalent per year (minimum 10.11, maximum 46.7 cm water equivalent). Analysis of a radargram from the site, with knowledge of this accumulation rate, indicated that reflectance horizons were not annual and that radar surveys with this frequency may not be suitable for gathering further snow accumulation data. The findings suggest that this triple ice divide is suited to glaciochemistry studies and that the retrieval of additional firn or ice cores, without melt influence, could contribute valuable data regarding the West Antarctic.

Contents

1.	Introduction.....	1
1.1	The West Antarctic Ice Sheet.....	1
1.2	Triple ice divides.....	3
2.	Accumulation Rate.....	5
2.1	Why investigate the accumulation rate?.....	5
2.2	Have others measured accumulation rates in western Antarctica?.....	5
3.	Determining annual layers.....	7
3.1	Density.....	7
3.2	Glaciochemistry.....	8
3.2.1	Major ions.....	8
3.2.2	Stable isotopes.....	11
3.3	Reference horizons.....	12
3.4	What others have found.....	12
4.	Methods.....	14
4.1	Study site.....	14
4.2	Sampling and preparation.....	14
4.3	Ion chromatography.....	15
4.3.1	Concept.....	15
4.3.2	Measurement procedure.....	16
4.4	Spectroscopy.....	17
4.4.1	Concept.....	17
4.4.2	Measurement Procedure.....	18
4.5	Radar.....	18
5.	Results.....	20
5.1	Density.....	20
5.2	Glaciochemistry.....	20
5.3	Radar.....	24
6.	Discussion.....	25
6.1	Seasonality.....	25
6.2	Climate variability.....	25
6.3	Anomalies.....	25
6.4	Lithium ions.....	27
6.5	Accumulation rate.....	27
7.	Conclusions.....	28
8.	Further research.....	29
9.	Acknowledgements.....	30
10.	References.....	31
11.	Appendix.....	37

1. Introduction.

The vast ice sheets of Antarctica are inherently influential. In the past, changes in ice sheets have had a significant influence on, and have been profoundly impacted by, global climate and ocean processes. Understanding their current dynamics is important to anticipating future instability and the potential for rapid change. It is of particular importance in the context of a changing climate.

The West Antarctic Ice Sheet (WAIS) has undergone significant retreat since the 1990s. It is theoretically unstable (Rignot et al. 2014) and any further ice sheet disintegration could pose significant implications for atmospheric, oceanic and cryospheric processes regionally and globally, including a rise in global sea levels. Since the 1950s, the West Antarctic has also been one of the most rapidly warming locations worldwide (Bromwich et al. 2012).

Despite receiving a lot of attention, knowledge of the WAIS remains limited. Computer models do not yet have the capacity to accurately simulate the ice sheet process so predictions of future rates of instability and retreat remain uncertain. It is beyond doubt that further research into the WAIS, including studies into snow accumulation rates and variability, is needed.

1.1 The West Antarctic Ice Sheet.

The WAIS is the continental ice sheet to the west of the Transantarctic Mountains, as shown in Figure 1. The WAIS contains around 10% of the ice volume of Antarctica, approximately 2.7 Million km³ of ice, which equates to over three metres of eustatic sea level rise if melted (Bamber et al 2009, Fretwell et al. 2013, Joughin & Alley 2011, Park et al. 2012). For this reason, if no other, it is of interest to understand more about the ice sheet.

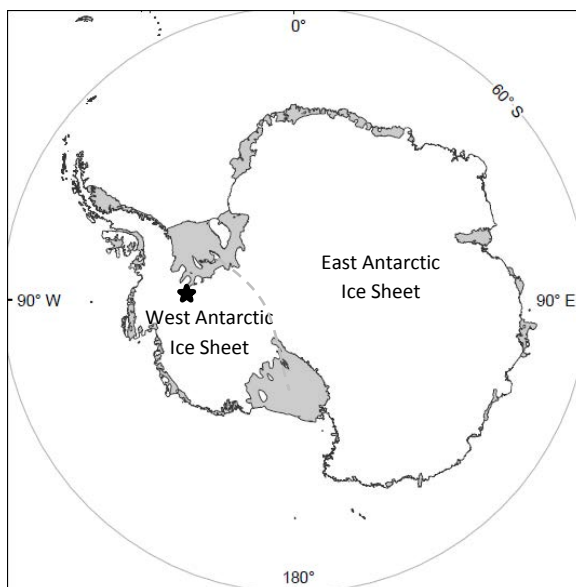
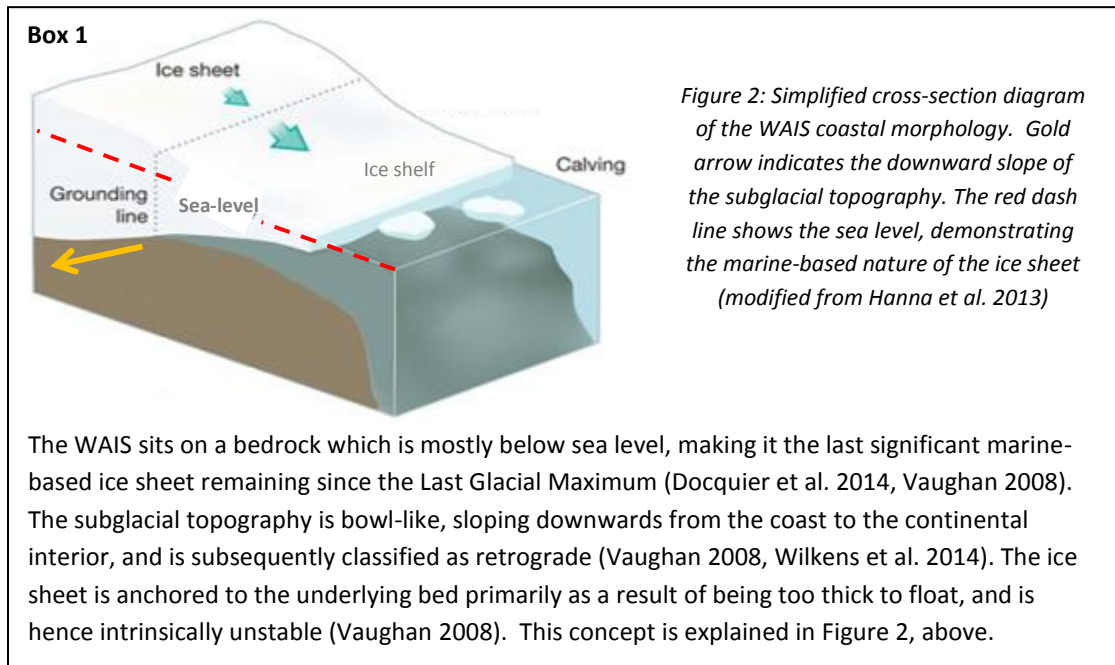


Figure 1: Map of Antarctic continent (black outline) and major ice shelves (grey shading) showing east and west Antarctic ice sheets. The black star indicates the study site. Based on map from the Australian Antarctic Division (AAD 2005).

The WAIS is classified as a marine-based retrograde ice sheet and is theoretically unstable (Bamber et al. 2009, Joughin & Alley 2011, Rignot et al. 2014). For more detail, see Box 1. A relatively small retreat could result in (gradual) ice sheet disintegration through a positive feedback between the

grounding line retreat and increased ice discharge (Gladstone et al. 2012, Wilkens et al. 2014). The coastal ice shelves which buttress the WAIS are vulnerable to the impact of changes in atmosphere and ocean temperature (Docquier et al. 2014, Dutrieux et al 2014, Joughin & Alley 2011). Due to this instability and its considerable ice volume, the WAIS has been identified as a possible tipping element, or threshold point, in larger-scale geophysical systems.



The availability of remote sensing imagery has confirmed changes in the WAIS. Satellite observations have revealed significant and increasing rates of mass loss from the WAIS, believed to be primarily due to thinning of coastal outlet glaciers into the Amundsen Sea over the past two decades (Docquier et al. 2014, Joughin & Alley 2011, Rignot 2014). In support of this finding, mapping of the grounding lines in the Amundsen Sea embayment, using radar interferometry, revealed major glacial changes in the 1990s, which have subsequently been confirmed with satellite radar altimetry, laser altimetry, feature tracking, ice thickness data and time-variable gravity (Rignot 2014, Mouginot et al 2013). These studies have led researchers to conclude that sections of the ice sheet remain unstable, with a lack of glacial bed obstacles to prevent further instability, and will contribute to sea level rise in the near future (Rignot et al. 2014).

In 1978, John Mercer first presented the idea of climate change-induced collapse of the WAIS causing worldwide catastrophe (Mercer 1978). Although the speed and magnitude of Mercer's proposed disintegration have been dismissed by many, in recent years the dynamics of the WAIS have again attracted substantial interest in academia, and in popular media, as regional instabilities have been realised (Vaughan 2008).

1.2 Triple ice divides.

Triple ice divides are the junctions at which three glacier divides meet. These locations, which often occur at summits, exhibit complex ice structures and dynamics to which normal ice flow assumptions and models cannot be applied (Hindmarsh et al. 2011). Improving our understanding of triple ice divides would be of benefit to the research of each of the three glaciers involved and the research of ice sheets more broadly. In recent years, ice-penetrating radar surveys of triple ice divides have been used to obtain more information on the glaciomorphology of these sites, which may then feed into ice flow models (Hindmarsh et al. 2011).

The triple ice divide of Pine Island Glacier, Institute Ice Stream and Rutford Ice Stream (PIR divide), located at the base of the Ellsworth Mountains, is the focus of this study. See Figures 1 and 3.

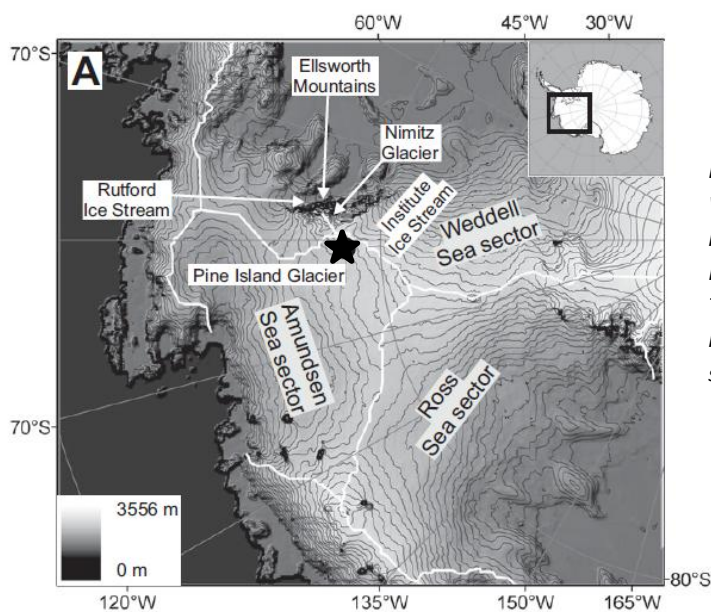


Figure 3: Ice surface elevation map of the WAIS with sectors and glaciers of interest labelled, including the Pine Island Glacier, Institute Ice Stream and Rutford Ice Stream. The black star indicates the approximate location of the PIR divide, the site for this study. Based on map from Ross et al. 2011.

Of the three PIR divide components, Pine Island Glacier (71°S, 100°W) is the most studied. It constitutes a major outlet into the Amundsen Sea (USGS 2014a) and has exhibited considerable acceleration, thinning and retreat in recent decades, leading it to be dubbed the ‘weak underbelly’ of the WAIS (Dutrieux et al. 2014, Hughes 1981, Gladstone et al 2012, Johnson et al. 2014). These recent changes have been attributed to an influx of warmer water under the ice shelf causing melting at the head of the glacier (Dutrieux et al. 2014, Johnson et al. 2014, Park et al. 2013, Wilkens et al. 2014).

The Rutford Ice Stream (79°S, 81°W) is around 290 km long and 25 km wide and sits in a deep, asymmetric, trough (Smith 1997, USGS 2014b). Refer to Box 2 for information on Ice Streams. Like the Pine Island Glacier, the Rutford Ice Stream is an important outlet of the WAIS. It drains ice from an area of high snow accumulation, around the Ellsworth Mountains, in a south east direction into the Ronne Ice Shelf (Goldstein et al. 1993, Smith 1997, USGS 2014b). Studies have shown the surface velocity of the Rutford Ice Stream to be highly variable, with variations of up to 20% on a fortnightly basis (Gudmundsson 2006).

Box 2. Ice streams are ribbon-like glaciers which flow at a faster rate than the adjacent ice (NSIDC 2014b). In Antarctica, ice streams are integral to the flow of ice from the interior, draining as much as 90% of the ice sheet (Goldstein et al. 1993, Smith 1997). Quantifying and understanding temporal variations in ice stream flows is necessary to estimating their past, present and future contributions to ice loss, and hence the contribution of the Antarctic ice sheets to global sea level changes (Gudmundsson 2006).

The Institute Ice Stream (82°S, 75°W) flows northwards into the Ronne Ice Shelf and is one of the largest glaciers in Antarctica in terms of width and outflow (Scambos et al. 2004, USGS 2014c). It has a significant role in draining the WAIS and understanding its behavior may be important to understanding the WAIS stability more holistically (Rippin et al. 2014). The Institute Ice Stream is susceptible to the influence of changes in the Pine Island Glacier drainage system.

Proximity of this triple ice divide to the Ellsworth Mountains, as indicated in Figure 3, is likely to influence precipitation at the site and the Mountains may also be a source of aerosols from evaporite dust (Dixon et al. 2005, Küttel et al. 2012).

The PIR divide is also believed to be located over a subglacial lake. A study into the regions' subglacial lakes has shown them to be more dynamic than previously known and subject to quite rapid changes which may influence the overlying ice sheets (Siegfried et al. 2014). There is still high uncertainty surrounding the implications of subglacial lake changes on the stability of overlying ice.

2. Accumulation Rate.

2.1 Why investigate the accumulation rate?

Knowledge of modern snow accumulation rates on the WAIS is limited to a sparse array of snow pit studies and instrumental measurements, which are generally confined to coastal regions and often do not capture the complexity of accumulation processes (Thomas et al. 2009). Knowledge of historic accumulation rates relies on a scarce - but growing - number of firn and ice cores (Siegert & Payne 2004). Firn and ice cores are invaluable sources of information for understanding the climatic trends of Antarctica, offering a wealth of palaeoclimate proxies, and can be measured across much of the continent (Thomas et al. 2009). Cores can provide a useful, high resolution, record of localised accumulation rates over century timescales which are used in the validation of climate and mass balance models and satellite observations (Banta & McConnell 2007, Kreutz et al. 2000). Snow accumulation is temporally and spatially variable, as explained in Box 3.

In western Antarctic, studies have concluded that global models tend to underestimate the magnitude of accumulation, in the Pine Island Glacier region (Medley et al. 2013). Accurate snow accumulation records from this region are paramount to improving models and understanding mass balance of glaciers and ice sheets (Banta & McConnell 2007, Ding et al. 2011, Spikes et al. 2004).

Box 3. The annual snow accumulation rate is the mass of snow or ice added to, and retained at, a given site per year (NSIDC 2014a). It is a function of gain through precipitation and snow drift, and loss through ablation processes such as surface melt.

Factors influencing the *temporal variability* of accumulation rates at a given site include annual changes in temperature, amount of precipitation, and the dynamics of poleward atmospheric moisture transport (Kaspari et al. 2004, Kreutz et al. 2000). Changes in cyclonic systems (eg. frequency, path, timing and strength) generally influence accumulation rates more than air temperature (Kaspari et al. 2004).

The *spatial variability* of accumulation rates is influenced by topography, altitude, and distance from moisture sources. Sites closest to the coast, or at lower altitudes, generally have the highest accumulation rates and those further from the coast, or at higher altitudes, receive less precipitation and have lower rates of accumulation (Kaspari et al. 2004, Kreutz et al. 2000). Coastal topographic features, such as mountains and valleys, are important to channeling the passage of moisture further inland.

2.2 Have others measured accumulation rates in western Antarctica?

Since the International Geophysical Year in 1957-58, research into the geophysical and glaciochemical parameters of Antarctica has increased substantially (Legrand & Mulvaney 1997, Vaughan 2008). Studies have sought to measure the accumulation rates of different sites based on snow pits, stake measurements, shallow firn cores and ice cores. Examples of these studies are provided in Table 1 and illustrate the substantial variability between sites.

Most results, but not all, conformed to the expected relationship between accumulation rate and both altitude and distance from the coast. Contrastingly, Kreutz et al. (2000) analysed data from 17 snowpits and cores, sampled across two transects on the WAIS, and found accumulation rates at three sites to show the opposite trend, illustrating the complexity of the responsible processes.

Table 1: Examples of previous accumulation rate measurements from Antarctica, sequenced by elevation. Grey shading indicates the two sites with elevations closest to the PIR divide site. w.e.: water equivalent.

Site	Altitude (masl)	Distance from open water (km)	cm yr ⁻¹ w.e.	Method	Citation
Siple dome	620	385	1.8	Ice core	Dixon et al. 2005
McCarthy Ridge	650		26	Firn core	Stenni et al. 2000
East Dronning Maud Land (H72)	1214		32.6	Ice core	Suzuki et al. 2005
Pine Island – Thwaites Drainage System, 01-6	1232	320	39.5	Ice core	Kaspari et al. 2004
Pine Island – Thwaites Drainage System, 01-5	1246	400	38.8	Ice core	Kaspari et al. 2004
Thwaites-Pine Island divide	1292	180	39	Firn core	Kaczmarak et al. 2006
Pine Island Glacier	1593		40.1	Ice core	Pasteris et al. 2014
West Antarctic plateau -B	1603		14.8	Ice core	Kreutz et al. 2000
Pine Island – Thwaites Drainage System, 01-3	1633	370	32.5	Ice core	Kaspari et al. 2004
James Ross Island	1640		40	Ice cores, snow pit samples	Aristarain et al. 2004
West Antarctic plateau A	1740		23.7	Ice core	Kreutz et al. 2000
WAIS (ITASE 00-1)	1791	475	2.3	Ice core	Dixon et al. 2005
Styx Glacier	1800	50	20.3	Firn core	Stenni et al. 2000
Thwaites Glacier	2020		27.3	Ice core	Pasteris et al. 2014
Taylor Dome	2365		6	Ice core	Monnin et al. 2004
Lambert Glacier	2390	310	10.9	Stake measurements	Ding et al. 2011
South pole	2850	1300	7.12	Snow pit	Whitlow et al. 1992
South pole	2850	1300	8.2	Ice core	Dixon et al. 2005.
EPICA	2900	500	7.7	Firn core	Isaksson et al. 1996
Vostok	3488		2.1	Snow pits	Ekaykin et al. 2002
Dronning Maud Land	3656		4.09	Snow pits	Hoshina et al. 2014
Dome Fuji	3810		2.5	Ice cores and snow pits	Iizuka et al. 2004
Dome Fuji	3785		2.93	Snow pit	Hoshina et al. 2014
Dome a	4093	1228	1.8-2.5	Stake measurements	Ding et al. 2011
West Antarctic Plateau		>400	14.4	Ground penetrating radar, ice cores	Spikes et al. 2004

3. Determining annual layers.

To determine annual snow accumulation rates from firn and ice cores, one must identify annual layers in the ice. There are various methods which can be used to establish the chronology of an ice core, their relative suitability dependent on the specific site. Methods analyse seasonal glaciochemistry cycles, stratigraphy, reference horizons, electrical conductivity measurements and radionuclides (Legrand & Mayewski 1997).

Multi-parameter layer counting, using numerous, robust, proxies in parallel, can increase the reliability of the chronology and account for possible errors in individual parameters (Anklin et al. 1998, Banta & McConnell 2007, Dansgaard et al. 1993, Legrand & Mayewski 1997, Schwikowski and Eichler 2010, Winstrup et al. 2013).

3.1 Density.

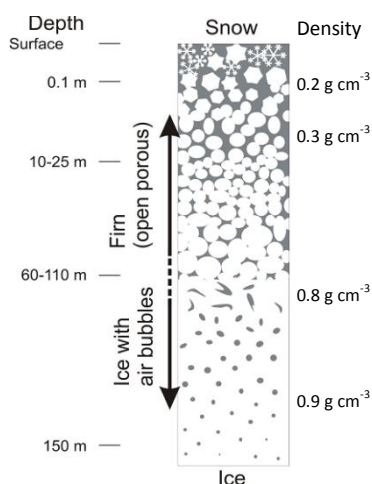


Figure 4: Densification of snow with depth. Image appropriated from University of Copenhagen Centre for Snow and Ice.

Density generally increases with depth in a glacier due to metamorphism driven by temperature gradients and the pressure of ensuing layers of snowfall, which expels air and causes deformation, as shown in Figure 4. The density-depth profile of a glacier uninfluenced by melt would therefore typically exhibit a gradual positive trend. Firn, which characterises the upper portion of glaciers, as shown in Figure 4, is defined in Box 4.

Density may be impacted by ice lenses, which are impermeable ice layers formed when surface melt occurs during the warmest part of the year and meltwater infiltrates the upper firn, refreezing and forming an impermeable ice layer (Kaczmarek et al. 2006, Olivier et al. 2003, Schwikowski et al. 2013).

Box 4. Firn is porous, well-bonded, snow which is older than one year and has a density of 200-800 kg m⁻³ (NSIDC 2014c). Near the surface of the accumulating snow, temperature gradients, which result from diurnal and seasonal variations, lead to evaporation and recondensation of water molecules, forming firn (Legrand & Mayewski 1997). At depth, firn is converted to ice through a densification process that gradually compresses the layers, removing air pores, and causing thinning deformation (Johnsen et al. 2000, Schwikowski et al. 2010, Schwerzmann et al. 2006).

3.2 Glaciochemistry.

Glaciochemistry is the study of the chemical parameters which are stored in, on and around, snow and accumulated in glaciers and ice sheets (Legrand & Mayewski 1997). Under suitable conditions, glaciochemistry can provide information about the composition of the atmosphere in the past, and changes in the sources, transport and distribution of various chemical species in the atmosphere (Kreutz & Mayewski 1999). It can also serve as a palaeothermometer. Specifically, glaciochemistry can provide information about the aerosol and water-soluble gas composition of the atmosphere when the ice was precipitated.

Ice from polar locations, particularly Antarctica, is of notable interest to glaciochemistry studies because of its geographical isolation. The isolation minimises local aerosol and gas sources such as dust, soil emissions and anthropogenic influence, resulting in a clean signal relative to many lower latitude sites (Dixon et al. 2005, Legrand & Saigne 1988, Legrand & Mayewski 1997). Polar meteorology also provides favourable conditions for ice records. The major seasonal cycle, of long polar nights with limited photochemical activity followed by long photochemically active summers, provides a sustained annual cycle (Legrand & Mayewski 1997).

3.2.1 Major ions.

Antarctic precipitation, and hence accumulating snow, consists of water with impurities. These impurities, which are mostly soluble species, are either primary aerosols introduced directly into the atmosphere or are secondary aerosols produced in the atmosphere through various oxidation pathways involving trace gases (Kreutz & Mayewski 1999).

There are a number of major ions retained in polar firn and ice. Their relative concentrations differ significantly between sites due to distance from sources, and the spatial and temporal variability of atmospheric circulation, sea ice extent, ocean productivity patterns and other factors (Sommer et al. 2000). The clarity of the signals at increasing depths also differs between ions (Kreutz & Mayewski 1999).

The two major sources of ionic species in Antarctic ice are sea salt and oceanic biogenic activity. Concentrations of sea salt ionic species usually peak in winter, coinciding with maximum sea ice cover (Hall & Wolff 1998, Röthlisberger & Abram 2009). Sea ice is coated in a fine layer of highly saline brine – termed ‘frost flowers’ – which is blown inland with strong winter winds (Kaspari et al. 2004, Richardson 1976, Hall & Wolff 1998, Röthlisberger & Abram 2009). The Antarctic winter exhibits more frequent advection of marine air masses over the ice sheet and increased storm activity, enabling transport of these species a long distance inland (Kreutz & Mayewski 1999, Legrand & Mayewski 1997, Suzuki et al. 2005).

Ionic species of biogenic origin usually peak in summer, when phytoplankton activity is high and sea ice cover is low in the Southern Ocean (Kreutz & Mayewski 1999, Stenni et al. 2000, Suzuki et al. 2005). It is believed that a more extensive winter sea ice cover promotes enhanced phytoplankton activity in the following summer (Röthlisberger & Abram 2009). Winter sea ice collects windborne dust and releases it to surface water with summer ice melt, providing nutrients for marine biota (Kaufmann et al. 2010). It is likely that a feedback exists between marine bioactivity, sulfate aerosols acting as cloud condensation nuclei, and cloud albedo – for example, the CLAW hypothesis - however

the nature of this interaction is a point of ongoing debate (Antony et al. 2010, Ayers & Cainey 2007, Charleston et al. 1987)

Chloride (Cl^-) can be measured directly in ice or calculated from Na^+ , as the Na^+ to Cl^- ratio is close to the sea water ratio at most sites. Cl^- is primarily from sea salt and the concentration subsequently declines with distance from the coast and with elevation (Mulvaney & Wolff 1994). At inland sites the Cl^- may exhibit seasonality different from the typical winter peak, due to Cl^- transport in upper troposphere air masses which are more likely to intrude over the continents interior in summer when there is greater downward mixing (Aristarian et al. 2004, Whitlow et al. 1992). As Cl^- as hydrochloric acid is volatile, it can sublime from snow into the atmosphere causing concentrations to change after deposition and caution should be taken when relying on this anion for layer counting (Iizuka et al. 2004).

Sodium (Na^+) in ice is usually a tracer of sea salt and generally displays a winter maximum with concentrations decreasing with altitude and distance from the coast (Kreutz & Mayewski 1999, Legrand & Mayewski 1997, Suzuki et al. 2005). Na^+ is often considered the most useful ion for identifying seasons due to the regularity of this cycle, particularly in coastal sites (Iizuka et al. 2004).

Calcium (Ca^{2+}), **potassium** (K^+) and **magnesium** (Mg^{2+}) concentrations in Antarctic precipitation are primarily from sea salt and can be used to study changes in atmospheric transport strength and sea ice cover. A component of these ions is also derived from terrestrial dusts, mainly from exposed bedrock surfaces in Antarctica and long-range transport from South America (Kreutz & Mayewski 1999). As larger aerosol particles, concentrations of these species are often believed to be dependent on accumulation rates, exhibiting dilution with high accumulation. In a reanalysis of glaciochemistry data from the WAIS, however, Ca^{2+} was the only ion which appeared to show statistically significant dependency on accumulation rate (Kreutz & Mayewski 1999). It is possible to partition sea salt and non-sea salt ion concentrations using Na^+ as the sea salt indicator (Whitlow et al. 1992).

Lithium (Li^+) is a trace ion which, similarly to Ca^{2+} , K^+ and Mg^{2+} can be derived from sea salt or dust. In sea water, lithium concentrations are relatively low and the Li^+/Na^+ ratio can be used to calculate the percentage from this origin (Siggaared-Andersen et al. 2002). Very few studies have analysed the lithium record from polar ice. A deep-core study at EPICA Dome C found Li^+ to be a mineral dust species deriving mainly from Bolivia (Siggaared-Andersen et al. 2007) and a Greenland study similarly found 95% of the Li^+ record to be of mineral dust origin (Siggaared-Andersen et al. 2002).

In Antarctica, **sulfate** (SO_4^{2-}) derives from sea salt and non-sea salt sources. Sulfate from non-sea salt origin (nssSO_4^{2-}) has three primary sources; volcanic eruptions, mineral dust, and oxidation of biogenic DMS. The latter source tends to dominate, with more than 75% of all sulfur emissions south of 35°S coming from marine origins (Sofon et al. 2014). Concentrations peak in summer, at most sites, rendering it as a useful chronology tool (Kaufmann et al. 2010, Mulvaney & Wolff 1994, Pasteris et al. 2014, Stenni et al. 2000). Concentrations of nssSO_4^{2-} have been shown to be independent from changes in accumulation rate and elevation but have a significant relationship to distance from coast, decreasing inland as the influence of lower-tropospheric air masses decreases (Dixon et al. 2005, Kreutz & Mayewski 1999, Mulvaney & Wolff 1994). Variability of nssSO_4^{2-} concentration at some WAIS sites has been linked to the sea ice extent in the Bellinghousen-Amundsen-Ross region (Dixon

et al. 2005). Studies have previously found a negative relationship between nssSO_4^{2-} concentrations and sea ice in the Pacific Ocean region, and a positive relationship to local polynia size (Dixon et al. 2005). In contrast to most nssSO_4^{2-} records, a study at Dome Fuji revealed a summer concentration minima (Iizuka et al. 2004). This was explained to be the result of summer post depositional processes, by which water sublimates from the upper snow layer during the day and condenses at night, resulting in a dilution. Iizuka et al. (2004) suggest that this mechanism may apply to other inland regions.

Methanesulphonate (CH_3SO_3^-), commonly referred to as Methanesulphonic Acid or MSA, is produced by the oxidation of phytoplanktonic dimethyl sulfide (DMS) and it is an unequivocal indicator of bioactivity (Stenni et al. 2000). Marine plankton produce DMS at the sea surface, which is released into the atmosphere and converted into MSA, sulfur dioxide, and other compounds (Kaufmann et al. 2010, Legrand & Saigne 1988). As such, Antarctic ice usually exhibits a summer MSA maximum. In some cases a winter MSA maxima has been recorded, which is proposed to result from post-depositional processes (Minikin et al. 1994, Stenni et al. 2000). In low accumulation areas, this post-depositional loss excludes it as a proxy of bioproductivity (Kaufmann et al. 2010). Changes in MSA concentrations measured in Antarctic ice may also result from low latitude climate conditions, such as insolation, sea temperature, surface temperature, and climate variability modes such as the El Niño Southern Oscillation, however little is known of these relationships (Kreutz & Mayewski 1999, Legrand 1997).

Ammonium (NH_4^+) presents a challenge to firn and ice core studies as it is very easily contaminated during sampling, processing and storage (Kaufmann et al. 2010). The source of NH_4^+ in Antarctica is not unequivocal, but it is likely to be of local biogenic origins. Particulate NH_4^+ is estimated to have a lifetime of less than one week and it is thus rapidly removed from the atmosphere during transport and, for inland Antarctica, this leaves the biomass production in the Southern Ocean as the most probable source (Kaufmann et al. 2010). A recent study has, however, found a strong relationship between black carbon and NH_4^+ concentrations in Antarctic ice, suggesting mid-latitude burning as a possible source (Pasteris et al. 2014). Concentrations are generally between 0.055 and 0.166 $\mu\text{eq/L}$ and tend to be highest in summer, with a less significant second peak in late winter or early spring at some sites (Kreutz & Mayewski 1999, Sommer et al. 2000). NH_4^+ concentrations are lower at higher elevations, and are not susceptible to post-depositional alteration (Kaufmann et al. 2010, Sommer et al. 2000).

The sources of **nitrate** (NO_3^-) in Antarctica remain unclear. Records generally show a peak in summer, which is believed to be due to the sedimentation and post-depositional redistribution of polar stratospheric clouds (PSC) and from tropical lightning (Pasteris et al. 2014, Mulvaney & Wolff 1993, Weller et al. 2011). It is hypothesized that PSC NO_3^- is precipitated in central Antarctica in winter-spring is then subject to summer post-depositional processes which result in its transportation in the polar boundary layer and precipitation at coastal sites (Mulvaney & Wolff 1993, Sofon et al. 2014, Weller et al. 2011, Wolff et al. 2008). The concentration in firn is therefore influenced by the location of the site, yearly PSC formation and sedimentation, sunlight and temperature of inland Antarctica, and air mass dynamics (Wolff et al. 2008). Concentrations tend to increase with altitude but decrease with accumulation rate (Kreutz & Mayewski 1999, Mulvaney & Wolff 1994, Traversi et al. 2014). As ozone depletion decreases with decreased PSC formation, it is possible that years with significantly depleted ozone could relate to decreased NO_3^- concentrations

(Weller et al. 2011, Mulvaney & Wolff 1993). For inland sites with low accumulation rates, the NO_3^- concentrations exhibit a steep decline in the upper 1 m of ice, suggesting slow-acting post-depositional processes and supporting the theory of NO_3^- re-emission (Mulvaney & Wolff 1994, Wolff et al. 2008). Over long time scales, NO_3^- in Antarctic ice can be used as a chemical tracer for variability in solar activity (Poluianov et al. 2014).

Fluoride (F^-) is a minor ion in most Antarctic firn records. The background concentration is usually measured at levels almost indistinguishable from zero - less than 0.01 $\mu\text{eq/L}$ (Hammer et al. 1997). Fluoride peaks have been recorded in deep ice cores at Dome C and Byrd Station, which indicate volcanic emissions from sources close to Antarctica in pre-historic times (Schwander et al. 2001, Vallelonga et al. 2005).

Formate (CHOO^-) in Antarctica is believed to derive from atmospheric oxidation of methane (Legrand & Saigne 1988). It is found in ice from both coastal regions and the central plateau, but is still usually a minor ion (Legrand & Saigne 1988).

Oxalate ($\text{C}_2\text{O}_4^{2-}$) in the atmosphere is primarily particulate matter which comes from forest fires, fuel combustion and soil emissions, or indirectly through photochemical reactions of hydrocarbons (Xinqing et al. 2002). As an aerosol in the form of oxalic acid it acts as a condensation nuclei and can accumulate in ice layers. Oxalate concentrations in Antarctica are generally very low with a maximum in spring and summer (Legrand et al. 1998).

3.2.2 Stable isotopes

Stable isotopes are atoms of the same element which have different numbers of neutrons, and therefore different masses, but which do not decay to other isotopes over geological timescales (Kendall & Caldwell 1998). Water molecules contain stable isotopes of hydrogen (H or D) and oxygen (^{16}O or ^{18}O). These are of use to palaeoclimatology because water molecules containing different isotopes behave differently during phase changes such as evaporation and condensation. Records which preserve the composition of water, such as glaciers, provide valuable information about the temperature conditions in which the molecules condensed. The mechanism responsible for this molecular separation is fractionation, explained in Box 5.

The ratio of the heavier ^{18}O isotopes to the lighter and more abundant ^{16}O is usually expressed as $\delta^{18}\text{O}$ as 'per mil' (‰), relative to the international standard, Vienna Standard Mean Ocean Water (vSMOW) (Craig 1961). Likewise, δD expresses the ratio of the less abundant D to the more abundant H, relative to vSMOW. The equation for calculation of the $\delta^{18}\text{O}$ value is provided below (Dansgaard 1964).

$$R = \frac{\text{amount of H}_2^{18}\text{O}}{\text{amount of H}_2^{16}\text{O}} \qquad \delta^{18}\text{O} = \frac{R_{\text{sample}} - R_{\text{standard}}}{R_{\text{standard}}} \cdot 1000\text{‰}$$

Stable isotopes of water are useful proxies as they are of unlimited volume in all firn and ice cores and they are not so liable to contamination during measurement (Dansgaard 1964). This method is, however, limited to upper layers and sites with high accumulation rates, due to the signal dampening

with depth through diffusion (Johnsen et al. 2000, Legrand & Mayewski 1997). Diffusion occurs through the inter-granular exchange of molecules in firn as vapour phase water, in which heavier isotopes are less abundant, moves through interconnected pores. The smoothing of the $\delta^{18}\text{O}$ profile is generally more pronounced than for the δD profile (Johnsen et al. 2000). Isotope records may also be impacted by post-depositional surface processes which impair the seasonal cycle (Hoshina et al. 2014).

Box 5. Isotopic fractionation is the enrichment of one isotope relative to another, and it occurs at each phase change of water. Molecules containing lighter isotopes are more volatile than those composed of heavier isotopes, causing fractionation during condensation and evaporation of liquid water (Dansgaard 1964, Legrand & Mayewski 1997). The isotope composition of H_2O in precipitation is highly dependent on the condensation temperature at which it is formed. Precipitation at colder temperatures is more depleted in heavier isotopes and has more negative $\delta^{18}\text{O}$ and δD values. Studying the isotopic signature of precipitation can reveal atmospheric temperature information (Dansgaard 1954, 1964, Ekaykin et al. 2002, NASA 2011b, Pfeiffer et al. 2004). Ice cores, which essentially record precipitation, subsequently provide a detailed proxy of temperature (Johnsen et al. 2000, Legrand & Mayewski 1997, Maselli et al 2013, Stenni et al. 2000).

3.3 Reference horizons.

Reference horizons provide an independent method for determining the age of specific layers within an ice core. This may be of use for confirming layer-count ages, for scaling ages, or for providing an age where accumulation rates may be too low for other methods (Legrand & Mayewski 1997). They are also a useful tool for cross-referencing between cores.

In Antarctic ice core records, major volcanic eruptions and bomb testing can provide reference horizons. Eruptions of Tambora (1815), Krakatoa (1883), Agung (1963) and Pinatubo (1991) are evident as nssSO_4^{2-} peaks at a 1-2 year lag to the eruption due to transport from low or mid-latitudes (Aristarian et al. 2004, Mulvaney & Wolff 1993). Tritium fallout from hydrogen bomb testing in 1963 is also used as a reference horizon, found in ice formed in 1966 (Aristarian et al. 2004).

3.4 What others have found.

There are still a limited number of annually resolved records of major ions and stable isotopes from firn and ice cores in Antarctica, but the availability of such records is growing (Medley et al. 2013). In non-coastal sites, seasonal oscillations in water stable isotopes, nssSO_4^{2-} , MSA and NO_3^- have most commonly been used to determine annual layers in firn and ice.

Water stable isotopes measurements from west Antarctica exhibit maxima in summer and minima in winter, with lower values at inland sites relative to coastal (Hoshina et al. 2014). Studies have found stable isotope variability in west Antarctica to be linked to large-scale atmospheric circulation, sea ice cover and local temperatures (Küttel et al. 2012). Various ion species have been found to vary seasonally in Antarctic sites and have been successfully used to count annual layers, such as those listed in Table 2.

In contrast to these studies, Iizuka et al. (2004) found that, in inland east Antarctica, the upper snow layer had a summer minimum in nssSO_4^{2-} and Na^+ concentrations, while exhibiting summer maxima of Cl^-/Na^+ , demonstrating that not all sites conform to the expected patterns.

Table 2: Examples of ion concentration parameters used for annual layer counting at different locations in Antarctica.

Site	Dating with:	Citation
South Pole	Na^+/Cl^- and nssSO_4^{2-}	Whitlow et al. 1992
Antarctic Peninsula	Summer nssSO_4^{2-} peak	Aristarain et al. 2004
Inland WA (A)	Summer nssSO_4^{2-} peak	Kreutz et al. 1999
Dronning Maud Land	Na^+ and Ca^{2+} peaks (winter-spring), NH_4^+ (2 months before Na^+)	Sommer et al. 2000
Dronning Maud Land	Na^+ and NO_3^-	Isaksson et al. 1996
Filchner Ronne Ice Shelf (acc. $>200 \text{ kg m}^{-2} \text{ a}^{-1}$)	Summer SO_4^{2-} peak	Manikin et al. 1994
Filchner Ronne Ice Shelf (acc. $100\text{-}200 \text{ kg m}^{-2} \text{ a}^{-1}$)	Summer SO_4^{2-} peak	Manikin et al. 1994
Dronning Maud Land	Summer MSA peak	Suzuki et al. 2005
Thwaites Glacier	Summer nssS/Na^+ peak	Medley et al. 2013
Northern Victoria Land	MSA and SO_4^{2-}	Stenni et al. 2000
Pine Island-Thwaites	Na^+ winter-spring peak and summer SO_4^{2-} and NO_3^- peak.	Kaspari et al. 2004
Siple Dome	Summer nssSO_4^{2-} peaks	Kreutz et al. 2000

4. Methods.

Methodologies for studying accumulation rates, and for analysing firn cores more generally, are now well developed and this study will follow existing procedures. The site selection and coring were undertaken prior to commencement of this thesis.

4.1 Study site.

The site for this study is the triple ice divide between Pine Island Glacier, Institute Ice Stream and Rutford Ice Stream in western Antarctica, described in Section 1.2, hereon referred to as the PIR divide. The firn core to be studied is 672 cm in length and was drilled at latitude 79°07'10.4339" S, longitude 88°50'21.0634"W, and altitude 2083.3 metres above sea level. The sampling was conducted on 18.01.2014 and the air temperature was -12°C. A 1000 km ground-penetrating radar transect and GPS data were also collected at the study site. Drilling and a radar survey were conducted by a team from the Centro de Estudios Científicos, Valdivia, Chile.

4.2 Sampling and preparation.

Preparation and storage of the frozen samples was in a -20°C laboratory, with attention paid to minimising contamination risk. For each of the 13 core segments, the following procedure was undertaken.

Core segments were weighed then removed from their packaging and placed onto a plexi-glass table. Segments were measured, and the lengths of individual sections of broken cores were recorded. The diameter was measured along the core and an average diameter estimated. The location and thickness of any ice lenses were recorded. Photographs were taken, with and without a backlight, and any additional structural features were noted.

The core segments were then prepared on a sterile, teflon, table which was fitted with a modified stainless-steel band-saw setup (Eichler et al. 2000). The outer parts of the ice core are usually contaminated during the drilling, handling, transport and storing processes, and this material was removed (Curran and Palmer 2001, Ivask et al. 2001). The ice was cut in a number of stages, as illustrated in Figure 5a, to produce a long rectangular piece of core, which was then cut into individual samples of 2.5-5 cm length, as in Figure 5b. Samples were placed into pre-cleaned and labelled airtight tubes, which were stored at -20°C until analysis.

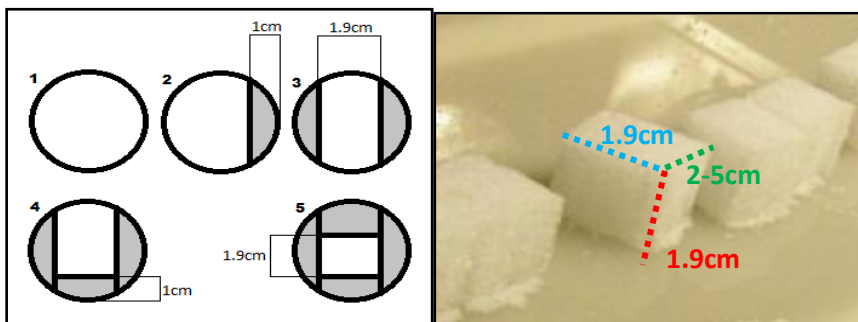


Figure 5a (left): Schematic showing the core cutting method, chronologically, for a cylindrical firn or ice core.

Figure 5b (right): Photo of individual samples cut from a firn core, with the approximate dimensions.

In total, 197 samples were cut.

Upon receiving the core segments at the Paul Scherrer Institut, it was discovered that segments of the core had been exposed to temperatures above freezing and had suffered some degree of melt. Melt layers appear transparent and bright when backlit, compared to unmelted segments, and often had a slightly deformed and non-cylindrical shape (Schwikowski et al. 2013). The extent of melt ranged from an estimated 20%, which could be effectively excluded from the samples, to almost 100% melt with severe deformity. Examples are provided in Figure 6. Where possible, samples were cut from the inner section of ice which appeared to be the least affected by this melt. It was expected that this melt-refreeze would have a significant impact on density measurements.

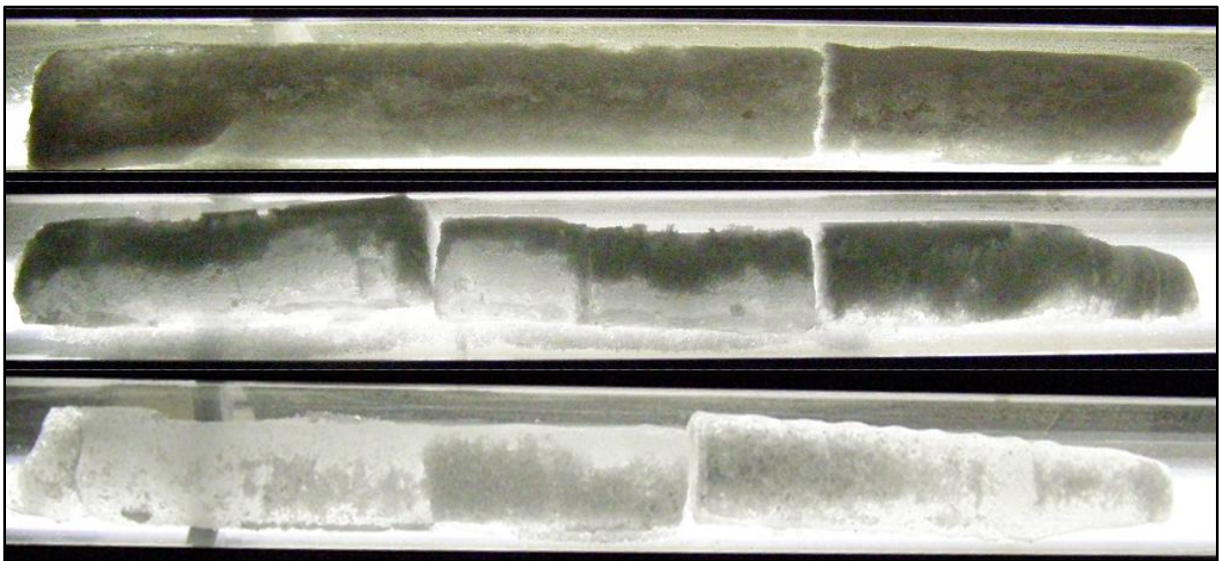


Figure 6: Backlit core segments; core segment 3 with limited melt (top), core segment 1 with moderate and inhomogeneous melt, and core segment 6 (bottom) with almost complete melt.

For chemical analysis, samples were removed from storage and tubes were immediately degassed using N₂ to remove laboratory air. The ice was melted and the tubes weighed. 500 µl of each sample was pipette into a vial for stable isotope analysis and the remaining sample was loaded into the ion chromatograph to be measured within the following 24 hours. After measurement, samples were frozen in storage.

4.3 Ion chromatography.

4.3.1 Concept.

Ion Chromatography (IC) is an analytical, physicochemical, method of separating ionic solutes in a sample and measuring their concentrations down to the parts-per-billion (ppb) range. It is a multispecies liquid chromatography technique which can be used to reliably quantify the concentration of a variety of ions simultaneously in a sample through a combined dual anion-cation process (Metrohm 2014). IC is widely used for determining ionic species from meltwater of snow and ice samples (Curran & Palmer 2001, Ivask et al. 2001).

The ion exchange method of IC is essentially based on the relative affinities of major anions or cations in a sample to their unique interactions with a resin. In brief, the method measures how long each ion species is retained in a resin column before it is replaced by an eluent ion and eluted. Ions with the lowest affinity, or the weakest ionic interactions, are the first to be eluted. This process is detailed in Box 6.

Box 6

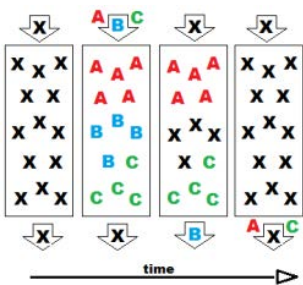


Figure 7: Schematic illustrating the concept of ion exchange in a resin column. X is an eluent ion. A, B and C are sample ions with different retention times.

The ion separation process occurs in a resin column. Initially, an appropriate eluent is injected into a charged, pressurised, chromatographic column (Bruckner 2013). The eluent ions exchange with and displace any other ions in the column, saturating the resin surface, and maintaining an electroneutral system. (See left column in Figure 7)

A sample containing ions of interest is then injected into the column. The sample ions exchange, one for one, with the eluent ions and bond to the surface of the resin (Bruckner 2013, Levin 1997). (See second column in Figure 7)

The sample ions are retained on the resin temporarily until the different ions are displaced, in an ion exchange, by eluent ions as more eluent is injected into the system (Metrohm 2014). Sample ions are then eluted from the column, and the time and concentration of ions released from the column are measured. (See third and fourth columns in Figure 7)

Each ionic species takes a different and known length of time to be eluted. Due to diffusion processes and the formation of flow channels in the column, not all ions of a single species will be released synchronously, and the IC peaks are subsequently Gaussian distributed (Metrohm 2014, UMM 2014).

4.3.2 Measurement procedure.

Ion chromatography was undertaken using a Metrohm 850 Professional IC with 872 Extension Module, as shown in Figure 8. The sample preparation and measurement methodologies were standard procedures for use of this equipment, and have been used regularly for experimentation and reliable measurements.

Eight anions were measured; fluoride (F^-), acetate (CH_3COO^-), formate ($HCOO^-$), MSA ($CH_3SO_3^-$), chloride (Cl^-), nitrate (NO_3^-), sulfate (SO_4^{2-}), and oxalate ($(COO)_2^-$).

Six cations were measured; sodium (Na^+), ammonium (NH_4^+), potassium (K^+), magnesium (Mg^{2+}), calcium (Ca^{2+}) and lithium (Li^+).



Figure 8: Metrohm Ion Chromatograph (left) and Autosampler (right). Image from Metrohm.

The measurement sequence contained blocks of sample measurements interspersed with standards and blanks (Milli-Q ultrapure water) to ensure that the measurement conditions remained constant.

All output graphs were reviewed, and baselines adjusted as necessary, to confirm that ion peaks were accurately identified and measured.

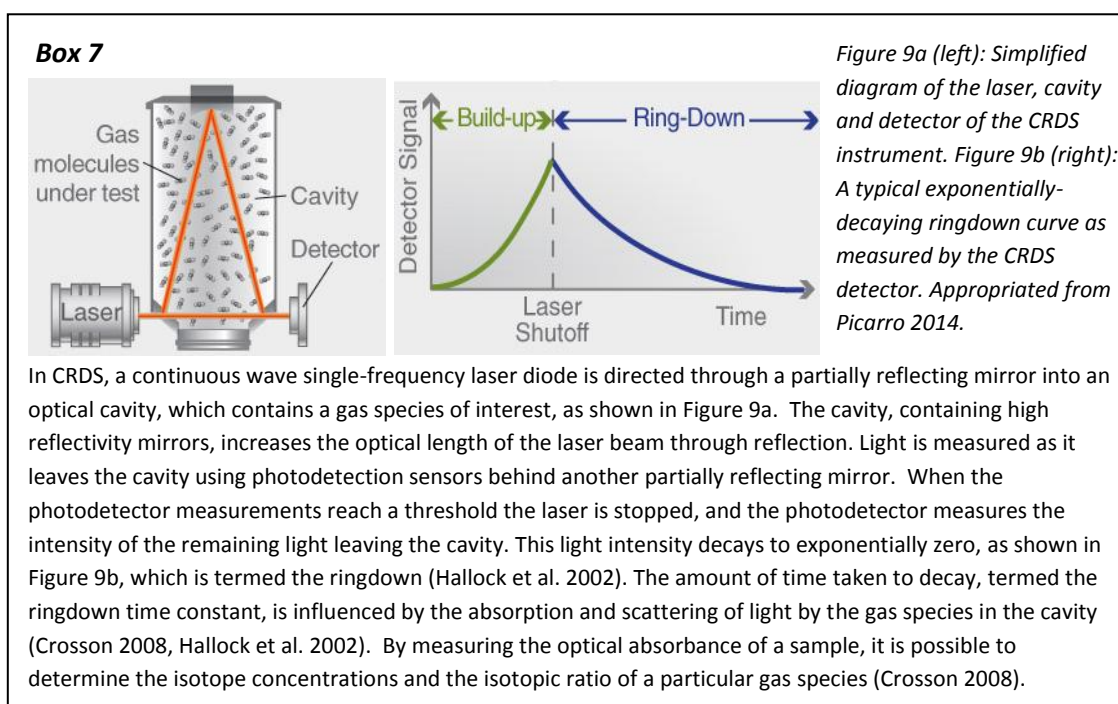
4.4 Infrared spectroscopy.

4.4.1 Concept.

The stable isotope analysis was undertaken using Wavelength-Scanned Cavity Ringdown Spectroscopy (WS-CRDS). WS-CRDS is an optical method using absorption spectroscopy with an infrared laser to measure the stable isotope concentration ratio of water in the vapour phase (Crosson 2008, Gupta et al. 2009). Infrared spectroscopy analyses differences in the vibration and rotation properties of molecules when interacting with light of infrared wavelengths. The method requires relatively little sample preparation, is quite efficient, and produces highly reproducible results, with high precision at very low concentrations compared to traditional mass spectrometry methods (Gkinis et al. 2010, Gupta et al. 2009). This method is detailed in Box 7.

The instrument is principally a gas-phase device. Liquid water is evaporated with a flash evaporation mechanism, and the resulting vapour is in equilibrium with a dry carrier gas to minimise isotopic fractionation upon phase change (Gupta et al. 2009).

Small gas-phase molecule species each have unique near-infrared absorption spectra. For each water molecule of different isotopic composition and weight, for example, highly specific spectral absorption features can be identified (Brand et al. 2009). By measuring the height of the absorption peaks one can measure the strength of the absorption, and hence the species concentration. CRDS is a technique which enables concentrations to be measured at low concentrations. (Picarro 2014)



4.4.2 Measurement Procedure.

Measurement of water stable isotopes was performed on a Picarro Cavity Ringdown Spectrometer L2130-I Isotopic H₂O instrument with a Vaporisation Module and auto-sampler. The methodology for use of this instrument, and data treatment, is well developed.

For each sample, six consecutive measurements were taken. The first three measurements were ignored and the second three, which were more stable and consistent, were averaged to provide the final value. In cases where one of the last three measurements was a clear outlier, the third measurement was used instead. Samples for which these three values had a standard deviation of greater than 10‰ for $\delta^{18}\text{O}$, or greater than 50‰ for δD , were re-measured. Samples were interspersed with standards and blanks to confirm the consistency of measurement conditions.

4.5 Radar.

Radargrams show discontinuities between successive layers in the material being measured. For the upper 75 m of a cold glacier, density variability has the greatest impact on radar reflectance (Winther et al. 1998). In snow-penetrating radar measurements, these reflectance horizons are often assumed to represent annual isochrones, caused by seasonal cycles of firn layers and associated ice crusts, and this assumption is commonly confirmed with the use of chemical analysis. Due to the high vertical resolution of modern radar measurements, it is possible to use the radar measurements for dating purposes, at sites where the annual cycles of conductivity can be confirmed, over depths and distances which may present challenges for ice core studies (Medley et al. 2013).

A study at Thwaites Glacier, for example, used chemical analysis to confirm the annularity of radar reflection horizons. Their study found that their radar provided accurate and independent estimates of accumulation rates across the study site, and was most accurate for accumulation between 30 and 60 cm w.e. yr⁻¹ (Medley et al. 2013).

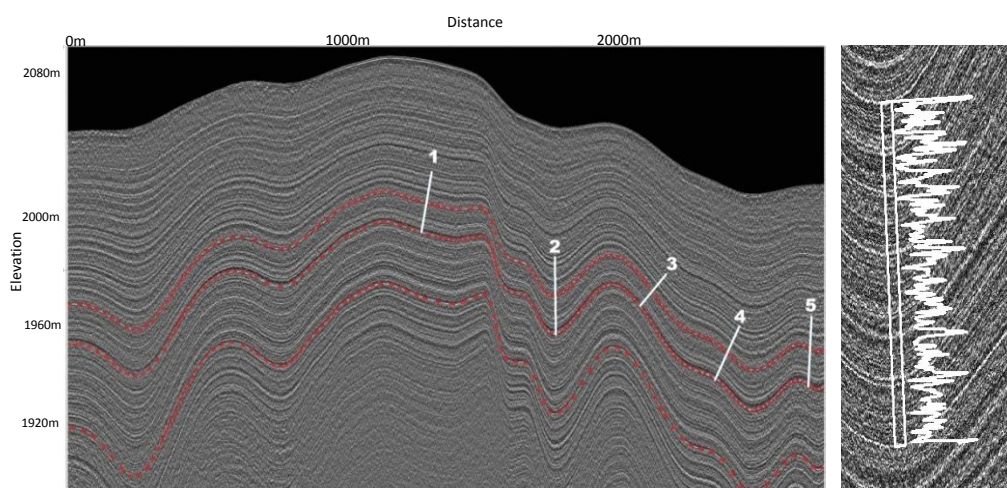


Figure 10a (left): Radar reflectance image from near the PIR divide, with red-dashed lines indicating the continuity of reflectance bands across the transect and solid white lines indicating the sections used to visually count reflections. Figure 10b (right): A section of the Figure 10a radargram is overlain with a line graph of the black-white contrast, produced using CoralXDS software.

For the PIR divide, the radargram was, similarly, analysed to estimate the number of reflectance horizons per metre of vertical depth, for comparison with the glaciochemistry results. The radar velocity was 194 m/ μ sec and had a resolution of 0.2 m in firn, with the uppermost 5 m obscured by alteration. Visual analysis was undertaken along five arbitrary lines, shown in Figure 10a, however the poor definition of individual reflectance horizons presented challenges to counting. In addition, a software program (Coral XDS), which was originally developed to identify annual banding in coral density images, was adapted for use on the black-white banding of radar imagery, producing a line graph which complemented the visual count, as shown in Figure 10b.

It is important to note that the measurement and processing of radar data occurred prior to this study, including the conversion from nanosecond return time to metres elevation.

5. Results.

5.1 Density.

The density profile for the PIR divide core, Figure 11, confirmed that significant post-drilling melting had impacted the majority of the core. A number of sections of the core had sample densities exceeding 0.8 g cm^{-3} which is the upper limit of firn, by definition, before it is classified as ice (NSICD 2014c). In comparison with the density profile of another Antarctic firn core, which was not subject to melting after drilling, it appears likely that most of the PIR divide core was influenced by some extent of melt.

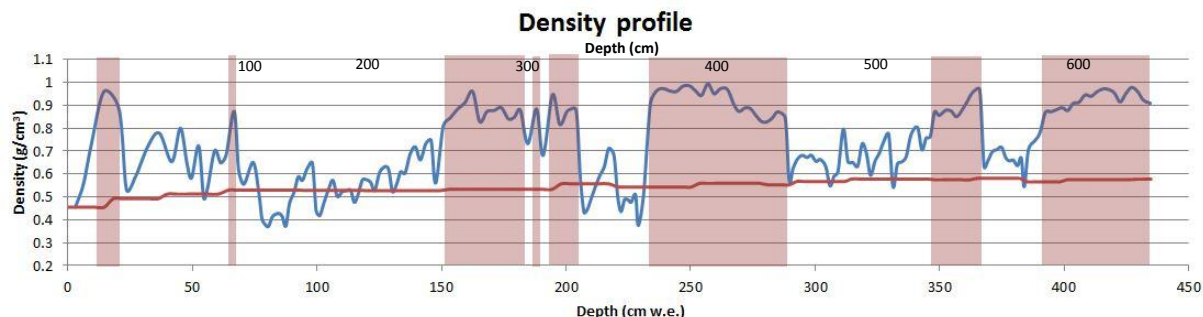


Figure 11: Blue line is the sample density for the PIR divide. The pink shading highlights the sections of this record which exceed 0.8 g cm^{-3} density, the upper limit of firn density. The red line is the core density of an Antarctic firn core undisturbed by melt, for the same depth in water equivalence. The sample density values have an error of around 0.085 g cm^{-3} .

The density measurements were, as such, not of use for annual layer counting, but were useful for identifying which segments of the core had been most influenced by this melting.

5.2 Glaciochemistry.

The stable isotope records of $\delta^{18}\text{O}$ and δD both displayed clear peaks and troughs, with maximum, minimum and mean values of -30.15 , -40.86 and -35.96‰ for $\delta^{18}\text{O}$, and -237.94 , -325.37 and -283.45‰ for δD . Based on visual analysis, $\delta^{18}\text{O}$ and δD values at around 250 cm water equivalent (w.e.) and 300cm w.e. depth had unclear peaks or troughs which may be due to impact by melt. As both isotope ratios showed the same pattern, only the $\delta^{18}\text{O}$ measurements, Figure 12, were used for analysis.

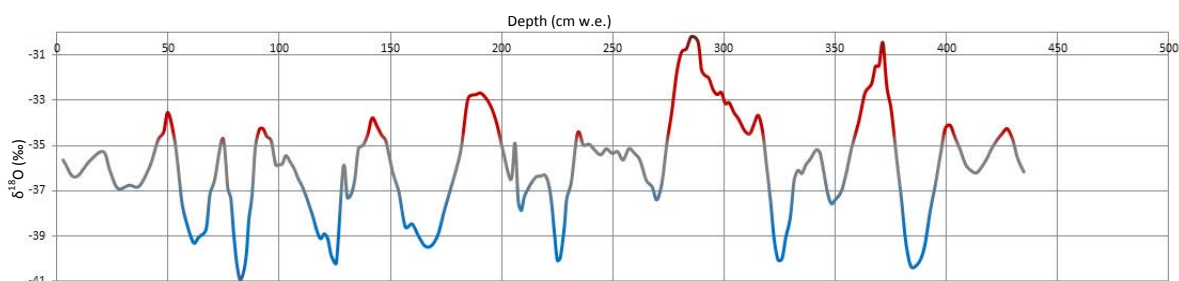


Figure 12: $\delta^{18}\text{O}$ record for the PIR divide firn core, with red and blue colours highlighting the high and low values.

The ion measurements also showed peaks and troughs throughout most of the records. For some ionic species the concentrations were close to, or below, the IC detection limits, such as $(\text{COO})_2^-$, or were deemed unreliable due to their susceptibility to contamination, such as NH_4^+ .

The concentrations of Cl^- , Na^+ , K^+ , MSA, SO_4^{2-} and NO_3^- , were deemed useful for analysis. For visual comparison of the ionic species, four point moving averages were calculated.

The nssSO_4^{2-} was calculated using sodium concentrations and the sea salt $\text{Na}^+ / \text{SO}_4^{2-}$ ratio (Mulvaney & Wolff 1994). These values showed that, on average, 78% of the total SO_4^{2-} was of non-sea salt origin. Therefore, the calculated nssSO_4^{2-} values closely followed the total values. Deuterium excess was calculated from the isotope measurements, using $\text{D-excess} = \delta\text{D} - 8(\delta^{18}\text{O})$ (Dansgaard 1964), and was in phase with the raw isotope data.

The ionic species was divided into two groups based on visual ‘wiggle’ matching. **Group 1 contained Cl^- , Na^+ and K^+** which appeared to be well aligned. These species all showed a high peak at 15cm w.e. depth and a particularly high peak, recorded across four samples, at around 150 cm w.e. depth. **Group 2 contained MSA, SO_4^{2-} and NO_3^-** which also aligned well together. These species also displayed the peaks at the two depths seen in group 1 however the second peak, at 150 cm w.e., was far less pronounced than in Group 1. The alignment of the ions in these two groups is evident in Figure 13. The ionic species in Group 2 all had a weaker (lower amplitude) signal after 300 cm w.e. depth, compared to their previous values, however the Group 1 species remained pronounced.

Correlation analysis was undertaken using the natural log values of the ionic species concentrations and the raw values of the isotope ratios. The results are given in Table 3. This confirmed the two ion groupings because the Group 1 ion Na^+ correlated (>70%) with Cl^- and K^+ , and the Group 2 MSA data correlated with SO_4^{2-} and nssSO_4^{2-} , and the SO_4^{2-} also correlated with NO_3^- .

Table 3: Correlation analysis of ions and isotopes measured in the PIR divide firn core. Colours highlight the correlations coefficients $r > 90\%$ (red), $r > 80\%$ (orange) and $r > 70\%$ (yellow). Ions which had low concentrations and were not useful to correlation studies were removed from the results table. The results show the highest correlation between oxygen isotope and hydrogen isotope records, followed by sodium-chloride, sulphate-nss sulphate, and sulphate-nitrate.

	$\delta^{18}\text{O}$	δD	fluoride	MSA	chloride	nitrate	sulfate	oxalate	sodium	potassium	magnesium	d-exc.
$\delta^{18}\text{O}$	1.00											
δD	0.99	1.00									90-100%	
fluoride	0.22	0.26	1.00								80-90%	
MSA	-0.04	0.02	0.24	1.00							70-80%	
chloride	-0.21	-0.19	0.19	0.34	1.00							
nitrate	0.09	0.11	0.12	0.68	0.40	1.00						
sulfate	0.03	0.07	0.14	0.80	0.45	0.80	1.00					
oxalate	0.03	0.06	0.78	0.28	0.14	0.11	0.18	1.00				
sodium	-0.24	-0.23	0.23	0.31	0.96	0.31	0.41	0.18	1.00			
potassium	-0.09	-0.05	0.29	0.33	0.65	0.26	0.37	0.30	0.72	1.00		
magnes.	-0.42	-0.40	-0.02	0.44	0.63	0.33	0.50	0.11	0.69	0.72	1.00	
d excess	0.06	0.18	0.40	0.54	0.11	0.25	0.29	0.22	0.11	0.29	0.10	1.00
nssSulf.	0.12	0.15	0.28	0.71	0.29	0.69	0.84	0.25	0.28	0.35	0.41	0.30

Principal Component Analysis was also undertaken to identify groupings of highly correlated ions. The results, shown in Table 4, confirm the two major groups.

	Component:1	Component:2	Component:3	Component:4	Component:5
fluoride	0.08	0.2	0.88	-0.16	-0.09
acetate	0.45	0.15	0.05	0.69	0.17
formate	0.35	0.47	0.48	0.47	0.02
MSA	0.91	0.14	0.12	-0.05	-0.14
chloride	0.2	0.92	-0.03	-0.06	0.2
nitrate	0.83	0.09	0.01	0.11	0.34
sulfate	0.87	0.2	0.04	0.08	0.2
oxalate	0.16	0.01	0.9	-0.05	-0.06
sodium	0.13	0.96	0.03	-0.01	0.16
ammonium	-0.12	0	-0.07	0.91	-0.1
potassium	0.08	0.77	0.26	0.29	-0.03
magnesium	0.25	0.26	0.03	-0.03	0.88
calcium	-0.14	0	0.79	0.27	0.29

Table 4: First five principal components based on a verimax rotation, using log-normalised data with anomalous samples removed from all ion data. Shading highlights the highest loadings for each component; red 90-100%, orange 80-90%, yellow 70-80%. Component 1 is mostly MSA, nitrate and sulphate. Component 2 is mostly chloride, sodium and

For multi-parameter annual layer counting it was of interest to find an alignment between the isotope measurements and the ion measurements. The ions of Group 2 were in phase with the isotope measurements, assumed to have maximum values in summer and minimum values in winter. The peaks and troughs corresponded particularly well from 0 to 225 cm w.e. depth. The ions of Group 1 were found to be inverse to the isotope values and were interpreted as having maxima in winter. The peaks and troughs of these Group 1 ions aligned particularly well with the isotope data from 300 cm w.e. depth onwards. These 'wobble' matches are shown in Figure 13.

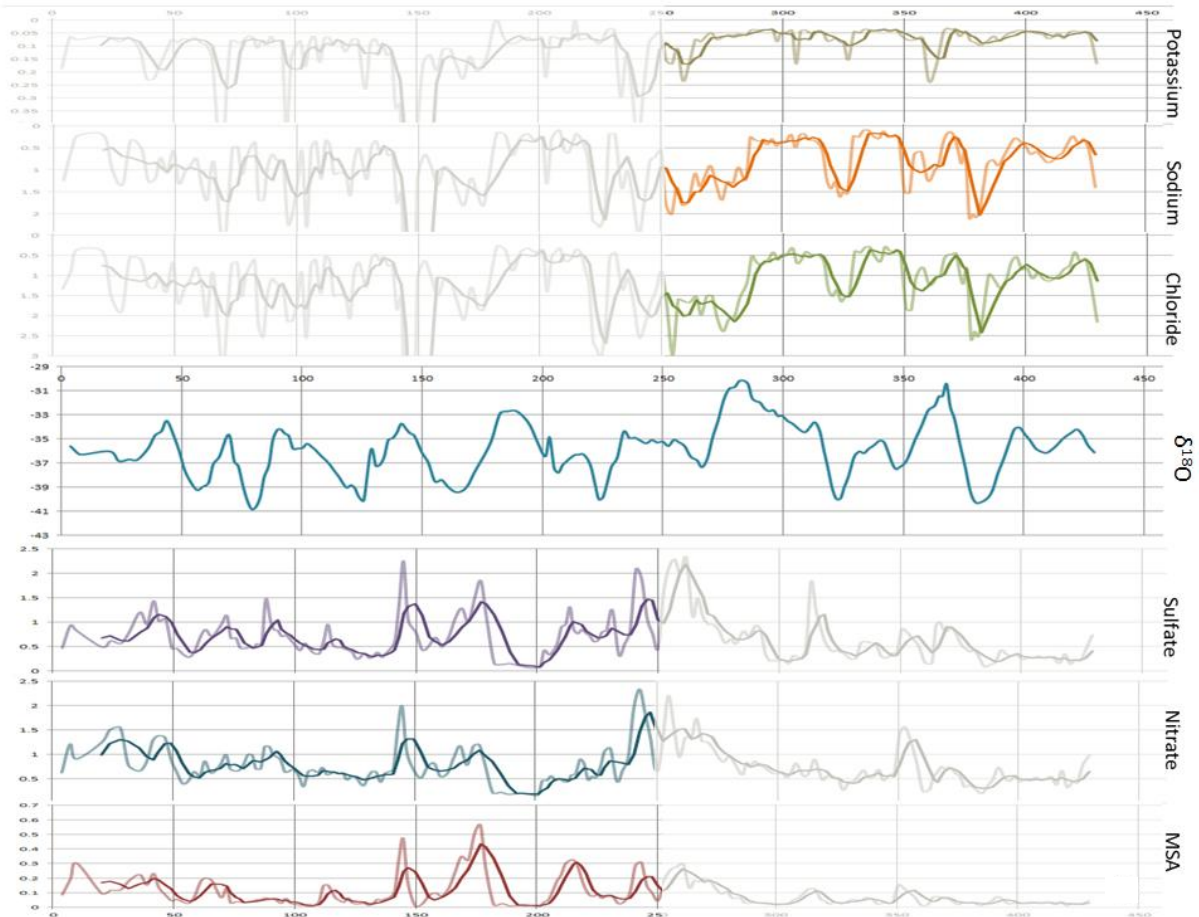


Figure 13: Wiggle-matching plot for major winter-peaking and summer-peaking ions relative to the oxygen isotope record for the PIR divide firn core. Ion concentrations ($\mu\text{eq/L}$) at four-point moving average, and raw $\delta^{18}\text{O}$ (‰) data. Note that the upper three ion graphs are inverted. X-axis is depth in cm water equivalent. Coloured segments indicate the sections of the ion records which best aligned with the $\delta^{18}\text{O}$ data.

The stable isotope ratios and ion concentrations for depths from 225 to 300 cm w.e. depth were more challenging to align visually. Referring back to Figure 11, these sections correspond to a segment of core with particularly high density and hence melt. For this section, the ion data was used to determine the most likely maxima and minima, as shown in Figure 14.

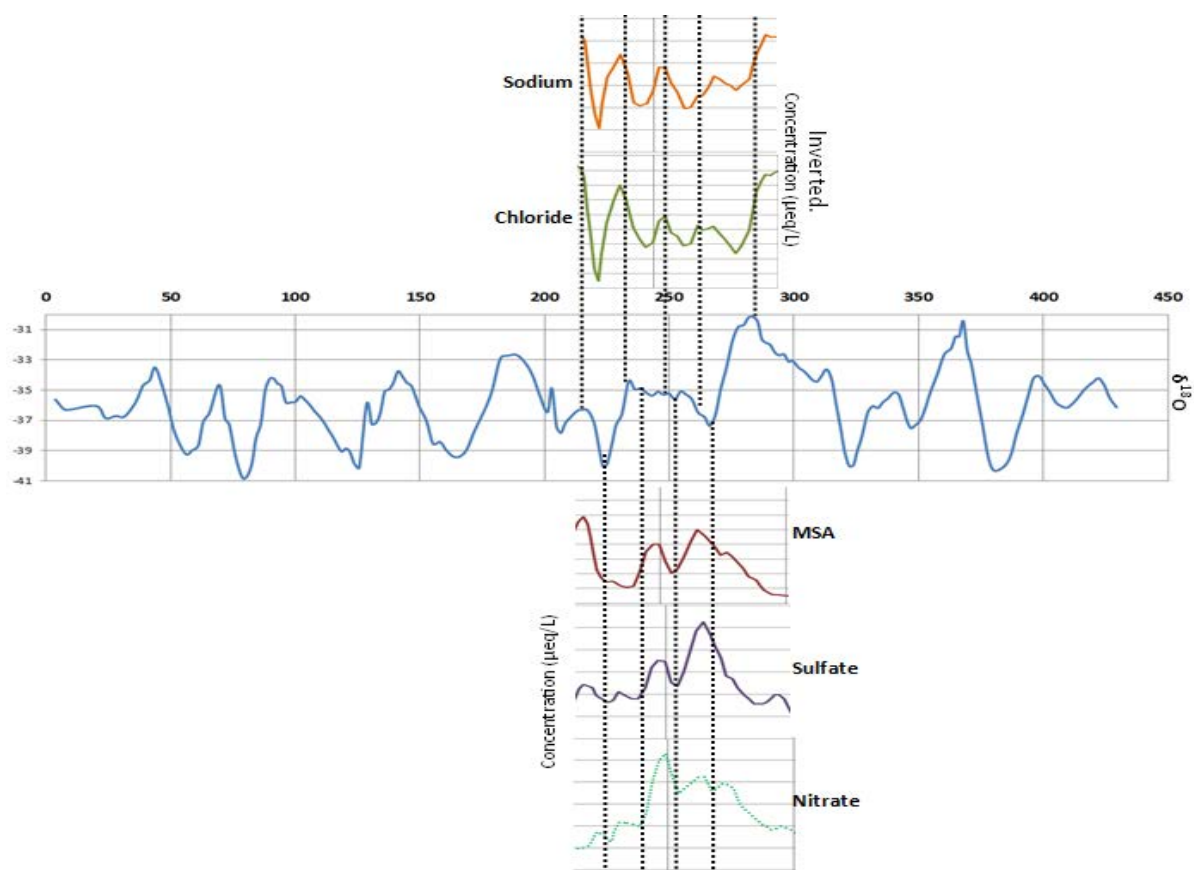


Figure 14: Wiggle-matching plot for major ion concentrations relative to the $\delta^{18}\text{O}$ (‰) for the PIR divide, focusing on the section from 200-300 cm w.e. depth where the peaks and troughs are not clearly defined. Ion concentrations ($\mu\text{eq/L}$) at four-point moving average, and raw $\delta^{18}\text{O}$ (‰) data. Note that the upper two ion graphs are inverted. X-axis is depth in cm water equivalent.

Based on the stable isotope ratios and ion concentrations, 18 summers were identified in the record – including the drilling season of summer 2013-2014. This is shown on the isotope record in Figure 15. It is important to note the uncertainty in the 225-300 cm w.e. section shown in Figure 14. Although 18 summer peaks is the best estimate with the available data, it is possible that the actual value is as low as 16 peaks.

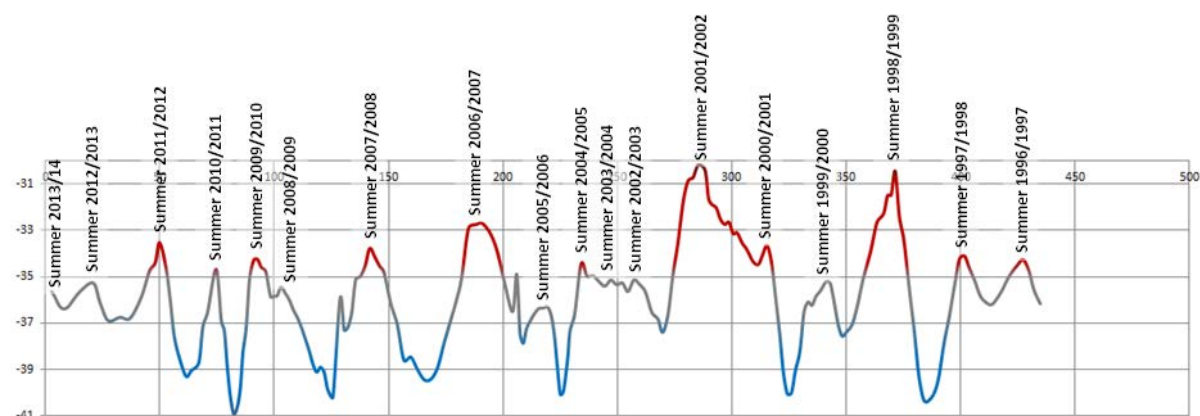


Figure 15: $\delta^{18}\text{O}$ measurements for the PIR divide with colours accentuating high and low values. Labels show austral summers based on annual layer counting. X-axis shows cm water equivalent depth, Y-axis shows $\delta^{18}\text{O}$ per mil.

With identification of annual peaks, it was possible to determine the snow accumulation per year through the core. Annual accumulation rates are shown in Table 4. The mean accumulation rate for this site is around 25 cm w.e. yr^{-1} with a range of 10.11-46.7 cm w.e. based on the number of years identified. An error of two years due to layer counting uncertainties would equate to an error

margin of approximately 3.5 cm w.e. on the average annual accumulation rate. Annual ion concentrations were also calculated for the major ions in this core. The average annual ion concentration was plotted against the annual accumulation rate to determine that ion concentrations were independent of accumulation rates.

Table 4: Annual snow accumulation rates and ion concentrations based on the years identified in the stable isotope and ion concentration records.

Accumulation rates and annual ion concentrations																	
Year*	2012	2011	2010	2009	2008	2007	2006	2005	2004	2003	2002	2001	2000	1999	1998	1997	MEAN
Accumulation (cm w.e.)	29.05	24.74	16.46	13.67	37.00	46.70	28.97	16.72	12.98	10.11	31.08	27.09	27.75	28.29	30.29	25.62	25.12
MSA ($\mu\text{eq/l}$)	1.26	0.96	0.58	0.26	1.13	3.66	1.59	1.11	0.88	0.49	2.16	0.61	0.79	0.83	0.60	0.30	1.13
Chloride ($\mu\text{eq/l}$)	8.67	14.61	14.32	13.18	20.61	33.16	7.26	15.58	9.22	7.06	22.83	8.16	13.04	11.63	20.33	9.84	14.08
Nitrate ($\mu\text{eq/l}$)	9.24	7.25	9.56	5.71	11.85	14.98	4.83	7.25	7.74	5.47	14.82	10.32	8.30	9.87	7.94	5.23	8.74
Sulfate ($\mu\text{eq/l}$)	7.09	6.27	8.01	5.26	8.82	16.47	6.26	7.56	6.42	4.97	15.65	7.85	7.95	7.25	7.09	2.77	8.03
Sodium ($\mu\text{eq/l}$)	6.61	12.33	10.25	10.90	16.31	29.98	5.32	11.97	7.64	5.06	17.21	4.87	10.91	9.08	14.83	6.35	11.06
Potassium ($\mu\text{eq/l}$)	1.04	1.40	1.05	1.18	2.31	5.42	1.02	0.89	1.24	0.43	1.16	0.8	0.94	1.08	1.00	0.59	1.34

* Year 2012 refers to the year from the austral summer 2011-2012 to the austral summer 2012-2013. Accumulation rates are calculated between consecutive summers, based on $\delta^{18}\text{O}$ peaks.

5.3 Radar.

The radargram analysis, both with and without the aid of software, identified approximately one radar reflectance band per vertical metre. The results of the counting, presented in Table 5 and Table 6, are highly uncertain due to challenges in band identification.

Based on the glaciochemistry results, above, and assuming an ice density of approximately 0.9 g cm^{-3} , one would expect an average of 4.4 years of accumulation in each vertical metre depth at this location.

Table 5: Number of radar reflectance horizons identified by eye in five transects on the PIR divide radargram. The transects were delineated into four segments of known vertical distance based on a few distinct horizons which were continuous across the entire radargram.

Number of radar reflection horizons counted: visual							
Vertical distance	Transect 1	Transect 2	Transect 3	Transect 4	Transect 5	Best estimate	Reflections per metre
6m (a)	8	7	6	7	6	7	1.16
6m (b)	3	8	5	6	3	5	0.83
10m	7	13	10	13	9	10	1.00
4m	3	4	5	2	3	5	1.25
Note: Best estimate based on counted values, weighted based on how defined reflections were in each section and in each transect.							Average: 1.06

Table 6: Number of radar reflectance horizons identified in four transects (different to those in Table 5) based on black-white contrast line graphs produced using Coral XDS from the PIR divide radargram.

Number of radar reflection horizons counted: software-assisted.						
Vertical distance	Transect A	Transect B	Transect C	Transect D	Average	Reflections per metre
44m	44	42	44	40	42.5	0.97

6. Discussion.

6.1 Seasonality.

The stable isotope data, with a $\delta^{18}\text{O}$ mean of -35.96‰ and δD mean of -283.45‰, are similar to those measured at other inland Antarctic sites, and lower than those at coastal and low altitude sites (Lorius et al. 1979, Stenni et al. 2000, Suzuki et al. 2005). The regularity of peaks and troughs throughout most of the timeseries suggests that the data is still suitable for use in counting annual layers.

The two groups of ions, confirmed through correlation analysis and principal component analysis, can be interpreted as reflecting two major sources. Group 1 (chloride, sodium, potassium) are ion species derived from sea salt and, to a lesser extent, from dust, which explains the maximum values in winter. The measured sodium to chloride ion ratio is very similar to the known sea salt ratio, as shown in Appendix 1, supporting that both ions are primarily from sea salt. Group 2 (MSA, sulphate, nitrate) are the summer-peaking ion species, primarily originating from biogenic activity of the southern ocean (excluding nitrate) with the concentration maxima in the austral summer. The nitrate signal may be derived from the re-deposition of PSC sedimentation which also occurs in summer.

6.2 Climate variability.

All ion and stable isotope time series contained variability which can be explained with variability in sources, year to year, and transport. This variability in sources and transport may, in turn, be explained by large scale climate variability. The ion and stable isotope data were compared with monthly data for the Southern Oscillation Index (SOI), the Antarctic Oscillation (AAO) and the Indian Ocean Dipole (IOD) to determine whether the anomalies or the magnitude of the peaks or troughs appeared to be driven by these climate variability signals. In general, there were no outstanding relationships visible. No statistical analysis was undertaken due to the short temporal duration of the measured record and dating uncertainty.

Records of Antarctic sea ice cover and cloud cover observations for the PIR divide region were, similarly, not found to align with the magnitude or anomalies of any ion concentrations or stable isotope ratio, based on visual analysis. Although these parameters unquestionably have an influence on glaciochemistry, it does not appear, for example, that the sea salt or biogenic ion variability is determined by sea ice cover or that the NO_3^- concentration are determined by insolation.

6.3 Anomalies.

Within the year-to-year variability of ion concentrations in the PIR divide firn core most values remained within a limited range. There were, however, two peaks in the raw ion data which appeared, visually, to be anomalously high. Potential explanations were investigated.

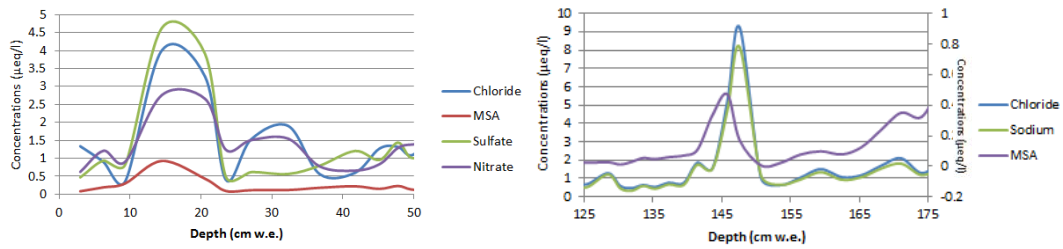


Figure 16: Examples of raw ion concentrations for two anomalous peaks in the PIR divide data. Figure 16a (left) peak is assumed to correspond to the 2012-13 austral summer and Figure 16b (right) is assumed to correspond to the spring of 2007 or summer of 2007-08.

The anomalous peak corresponding to summer 2012-2013 in the raw ion data (not clear in the 4pt moving average) occurs in all major ions and is particularly high, based on visual analysis, in the records of SO_4^{2-} , NO_3^- , MSA, Cl^- , formate, oxalate, F^- , Mg^{2+} . Figure 16a shows this peak in four ion records.

The peak is challenging to explain as it is evident in ions from various sources including summer and winter peaking ions. In the SO_4^{2-} record, a potential source would be the 2011 Puyehue-Cordón Caulle eruption in Chile ($40^\circ 35' 25''\text{S}$ latitude) which caused ash fallout in much of the southern hemisphere (Smithsonian Institute 2013). To link this eruption to all other ions through the indirect impacts of ash deposition, temperature decrease, insolation decrease and subsequent sea ice impacts, is challenging. No significant impacts of the 2011 eruption on these parameters have been documented. A peak in NO_3^- could be explained as resulting from an anomalous stratospheric air intrusion, however this source does not apply to other ions (Traversi et al. 2014). More likely, a strong wind event from the coast could have caused an increase in species. Hall and Wolff (1998) found that the highest sea salt concentrations at their study site were associated with changes in wind direction, on the day of or the day before the measured peak. It is, however, questionable that this would cause so many ions to peak simultaneously.

A possible explanation is therefore that this peak, which occurs over two samples for most ions, is the result of melt water accumulating at this point in the core. The samples were on either side of a break point in a melted core segment and it is possible that the water, which melted during transport, refroze in this break, concentrating the ion species. This explanation is supported by a higher density measured in these samples.

The anomalous peak corresponding to late 2007, Figure 16b, is most pronounced across sea-salt species but also appears to a lesser extent in summer-peaking species. This could be interpreted as resulting from a single transport event which caused an influx in salt-enriched air masses to this site. Due to the limited spatial and temporal resolution of weather observations for this region it is challenging to find a record of this event. Monthly and seasonal surface wind and sea level pressure records were examined for anomalies however none prevailed.

Monthly records of Cl^- concentration at the Thwaites and Pine Island Glacier divide, based on a shallow firn core, recorded a maximum value of $28.5 \mu\text{eq/L}$ in March 2008 – around eight times the mean value and double the second and third highest values measured, 2002-2010 (Crisciello et al. 2013). This falls very near, temporally, to the PIR divide peak, as shown in Appendix 3. It is possible that the peak in each dataset is from the same event and appears at a slightly different time in the

PIR divide core due to dating uncertainty. Melt may also have influenced the position of the ion peak. Monthly MSA values measured in the same core showed a maximum in November and December of 2007, closer to the PIR divide peak, however these values were not as anomalously high. The Cl⁻ record in the Criscitiello et al. (2013) study was found to have a strong positive correlation with the winter sea ice cover in the Amundsen Sea polynia. More detail of polynias is provided in Box 8.

Box 8: Polynias are sea surface areas with reduced sea ice cover, located in regions which would be expected to have, and are surrounded by, substantial sea ice cover (Arrigo & van Dijken 2003, Criscitiello et al. 2013). These polynias often result from local wind patterns and can increase winter sea salt aerosols due to the high, ongoing, rate of brine-enriched sea ice formation which is subjected to continuous wind dispersal (Criscitiello et al. 2013).

Although polynias are a winter phenomenon, it is the spring and summer manifestations of these areas (termed post-polynias) which attract the most attention (Arrigo & van Dijken 2003). Post-polynias are the first areas in which the sea surface is exposed to the increasing spring insolation and they are subsequently the sites of very high bioproductivity (Arrigo et al. 2012, Arrigo & van Dijken 2003, Criscitiello et al. 2013, Dixon et al. 2005). Three of the four most productive polynias in Antarctica are in the west Antarctic. The Pine Island Bay polynia, is noted as being particularly productive (Arrigo et al. 2012, Dixon et al. 2005). The total January productivity of all the polynias in Antarctica is around three times that of the surrounding Southern Ocean (Dixon et al. 2005).

6.4 Lithium ions.

The Lithium ion record was of particular interest as most samples contained no measurable concentration however in a few samples it peaked very clearly. These few peaks aligned with winter-peaking ions, such as K⁺, and it is assumed that the measured Li⁺ comes from sea salt and dust. It is unclear what would cause the lithium to appear only four times in the core, as these occurrences did not appear to coincide with notable events in the climate variability modes discussed in Section 6.2.

The most defined Li⁺ peak was in early 2009, with another less defined peak in early- to mid-2008. The summer of 2008-09 had, simultaneously, strong positive phases of both the Southern Oscillation index and the Southern Annular Mode (Tedesco & Monaghan 2009), however this was not the case in the previous year and it is not a clear cause for these peaks. Low sea ice cover was measured in west Antarctic polynias in the austral summers of 2002/03, 2007/08 and 2009/10 which may provide a better explanation for the Li⁺ peaks but is far from equivocal (Criscitiello et al. 2013). In 2009 the Antarctic snowmelt index (number of melting days times the melt area) set a new historical minimum based on the period 1980-2009 but this does not relate to earlier Li⁺ data (Tedesco & Monaghan 2009).

With so little Li⁺ data, and no outstanding correlation to climate events, the cause of the Li⁺ variability remains undetermined.

6.5 Accumulation rate.

The mean accumulation rate for the site, around 25 cm w.e. yr⁻¹, is within the range of other data from sites in the region. In particular, these values are similar to those obtained from a firn core at Styx Glacier at a similar altitude; 20.3 g cm⁻² yr⁻¹ (range of 11.1-33.5 g cm⁻² yr⁻¹) (Stenni et al. 2000).

With the available resolution of the radargram it was challenging to reliably count the reflectance horizons. The best possible interpretations of the data found an average of around one horizon per vertical metre of depth. Based on this, it is not possible to align reflectance horizons with annual layers at this site. This would imply that researchers must rely on further firn and ice core studies to, or rely on radar data of higher frequency, to extend accumulation rate data in the region. If additional radar images of higher resolution were available, it may be possible to more accurately count horizons and determine accumulation rates.

7. Conclusions.

The WAIS is theoretically unstable and many of its glaciers have retreated in the past two decades. Although significant advances have been made in understanding and modelling climate and glacial processes in the region, much remains unknown. The triple ice divide between Pine Island Glacier, Institute Ice Stream and Rutford Ice Stream on the WAIS is of particular interest to glaciologists because a substantial volume of west Antarctic ice drains via these three glaciers. At present, little is known of the accumulation rate in the region, and a better understanding of this may improve knowledge of ice flow and of WAIS stability, more broadly.

The shallow firn core drilled at the PIR divide was severely impacted by post-drilling melt. Nonetheless, the ion and stable isotope measurements proved suitable for annual layer counting, with seasonal cycles evident in the stable isotope time series and in both the summer- and the winter-peaking species. Sea salt and dust related species were found to peak in winter and the biogenic species and nitrate were found to peak in summer, a result which agrees with many other studies. The accumulation rate was calculated to be around 25 cm w.e. yr⁻¹ based on the 18 summer peaks identified. This value could differ by up to two years, due to melt-related uncertainties, which would result in a different annual accumulation rate.

It does not seem likely that the radargram reflectance horizons are annual, based on the calculated accumulation rate and accounting for a melt-induced error margin. As such, the PIR divide radargram is not suitable for analysing accumulation rates over greater spatial and temporal ranges.

Variability in the amplitude of ion concentration peaks did not appear to align clearly with any particular climate parameter. Anomalous peaks in ion concentrations have been seen in similar studies and are most likely resulting from short-lived weather events or from melt influence in the core.

This site is well located for studying WAIS dynamics, and the results of this study indicate that the ion and stable isotope data are seasonally cyclic and useful for annual layer counting. This site may, subsequently, offer more research possibilities in the future.

8. Further research.

Despite the enormous advances which have been made in Antarctic climate studies, the current distribution of firn and ice cores undersamples the spatial variability of the continent (Medley et al. 2013, Siegert & Payne 2004, Spikes et al. 2004). As such, any additional accumulation rate information is advantageous. Data pertaining to the WAIS, and specifically to complex junctions such as the PIR divide, is necessary to better understand and model glacial flow and stability.

Specific to the PIR divide site, it would be beneficial to obtain another core to analyse without the influence of melt. From this, accumulation rates could be measured with greater certainty. There were no distinct index horizons through this firn core. Based on the average annual accumulation rate that was measured and assuming, conservatively, a firn density of 0.350 g cm^{-3} , further cores at this site could be drilled to over 959.1 cm depth (287.1 cm beyond this core) to reach the 1992-93 austral summer where the Pinatubo eruption (1991) should register (Hoshina et al. 2014). This would provide confirmation of accumulation rate measurements.

In addition, a higher resolution radargram could be measured to better confirm the relationship between reflectance and annual layers. If reflectance horizons were found to correspond with years of snow accumulation, then the accumulation rates could be identified over greater distances and depths.

There is endless scope for further research in this little-known region of the world, but more accumulation rate data is a good place to begin.

9. Acknowledgements

This thesis is the work of 'Fenwick et. al.'. It reflects the hard work of many.

Central to this project was the firm core itself. The core was drilled by Dr Andres Rivera and his colleagues at the Centro de Estudios Cientificos, Chile, who provided it to PSI for analysis. The opportunity to analyse this core was made possible by Dr Margit Schwikowski, my Supervisor, to whom I am endlessly grateful for allowing me to work on the project.

I also owe big thanks to Sabina Brüttsch who makes the instruments dance and took the time to show me the steps. Likewise, I am hugely thankful to Dr Anja Eichler who cut the core and helped me, with unbelievable patience, throughout the whole project.

The University of Bern enabled me to undertake this project within my Master's program, and the Laboratory of Radio Chemistry and Environmental Chemistry at the Paul Scherrer Institute welcomed me to use their facilities and their brains, and allowed me through the security gates each and every day.

This thesis project has been a dream opportunity, and I am indebted to everyone who made it possible.

Vielen Dank für die Erklärung des *K's* für *Potassium* und des *Na's* für *Sodium*!

10. References

- AAD: Australian Antarctic Division (2005) Australian Antarctic Data Centre –Map 13202, https://data.aad.gov.au/aadc/mapcat/display_map.cfm?map_id=13202
- Arrigo K, van Dijken G. 2003. Phytoplankton dynamics within 37 Antarctic coastal polynya systems. *Journal of Geophysical Research*. 108: 3271-3289
- Arrigo K, Lowry K, van Dijken G. 2012. Annual changes in sea ice and phytoplankton in polynyas of the Amundsen Sea, Antarctica. *Deep Sea Research Part II: Topical Studies in Oceanography*. 71–76: 5–15
- Aristarain A, Delmas R, Stievenard M. 2004. Ice-Core Study Of The Link Between Sea-Salt Aerosol, Sea-Ice Cover And Climate In The Antarctic Peninsula Area. *Climatic Change*. 67: 63–86
- Ayers G, Caine J. 2007. The CLAW hypothesis: a review of the major developments. *Environmental Chemistry*. 4: 366–374.
- Bamber J, Riva R, Vermeersen B, LeBrocq A. 2009. Reassessment of the potential sea-level rise from a collapse of the West Antarctic Ice Sheet. *Science*. 324: 901–903
- Banta J, McConnell J. 2007. Annual accumulation over recent centuries at four sites in central Greenland. *Journal of Geophysical Research*. 112
- Brand W, Geilmann H, Crosson E, Rella C. 2009. Cavity ring-down spectroscopy versus high-temperature conversion isotope ratio mass spectrometry; a case study on $\delta^2\text{H}$ and $\delta^{18}\text{O}$ of pure water samples and alcohol/water mixtures. *Rapid Communications in Mass Spectrometry*. 23: 1879–1884.
- Bromwich D, Nicolas J, Monaghan A, Lazzara M, Keller L, Weidner G, Wilson A. 2013. Central West Antarctica among the most rapidly warming regions on Earth. *Nature Geoscience*. 6: 139-145.
- Bruckner M. 2013. Ion Chromatography. Science Education Resource Centre at Carleton College, Montana State University, http://serc.carleton.edu/microbelife/research_methods/biogeochemical/ic.html (accessed 21/08/2014)
- Charlson R J, Lovelock J E, Andreae M O and Warren S G 1987 Oceanic phytoplankton, atmospheric sulphur, cloud albedo and climate *Nature* 326 655–661
- Craig H. 1961. Isotopic Variations in Meteoric Waters. *Science*. 133: 1702-1703
- Crisciello A, Das S, Evans M, Frey K, Conway H, Joughin I, Medley B, Steig E. 2013. Ice sheet record of recent sea-ice behavior and polynya variability in the Amundsen Sea, West Antarctica. *Journal of Geophysical Research*. Oceans. 118
- Crosson E. 2008. A cavity ring-down analyzer for measuring atmospheric levels of methane, carbon dioxide, and water vapor. *Applied Physics B*. 92:403–408.
- Curran M, Palmer A. 2001. Suppressed ion chromatography methods for the routine determination of ultra low level anions and cations in ice cores, *Journal of Chromatography*, 919: 107–113
- Dansgaard W. 1954. The O16 abundance in freshwater. *Geochimica et Cosmochimica Acta*, 6: 241-260
- Dansgaard W. 1964. Stable isotopes in precipitation. *Tellus*, 16: 436-468.
- Ding M, Xiao C, Li Y, Ren J, Hou S, Jin B, Sun B. 2011. Spatial variability of surface mass balance along a traverse route from Zhongshan station to Dome A, Antarctica. *Journal of Glaciology*. 57: 658-666
- Dixon D, Mayewski P, Kaspari S, Kreutz K, Hamilton G, Maasch K, Sneed S, Handley M. 2005. A 200 Year Sulfate Record from Sixteen Antarctic Ice Cores and Associations With Southern Ocean Sea-Ice Extent. *Annals of Glaciology*. 41: 155-166
- Docquier D, Pollard D, Pattyn F. 2014. Thwaites Glacier grounding-line retreat: influence of width and buttressing parameterizations, *Journal of Glaciology*, 60: 305-313
- Dutrieux P, Rydt J, Jenkins A, Holland P, Kyung Ha H, Hoon Lee S, Steig E, Ding Q, Abrahamsen E, Schroder M. 2014. Strong Sensitivity of Pine Island Ice-shelf Melting to Climatic Variability. *Science*. 343: 174-178

- Eichler, A., Schwikowski, M., Gäggeler, H.W., Furrer, V., Synal, H. A., Beer, J., Saurer, M., and Funk, M.: Glaciochemical dating of an ice core from upper Grenzgletscher (4200ma.s.l.), *J. Glaciol.*, 46, 507–515, 2000.
- Ekeykin A, Lipenkov V, Barkov N, Petit J, Masson-Delmotte V. 2002. Spatial and temporal variability in isotope composition of recent snow in the vicinity of Vostok station, Antarctica: implications for ice-core record interpretation. *Annals of Glaciology*. 35: 181-186
- Fretwell P, Pritchard H D, Vaughan D G, Bamber J L, Barrand N E, Bell R, Bianchi C, Bingham R G, Blankenship D D, Casassa G, Catania G, Callens D, Conway H, Cook A J, Corr H F J, Damaske D, Damm V, Ferraccioli F, Forsberg R, Fujita S, Gim Y, Gogineni P, Griggs J A, Hindmarsh R C A, Holmlund P, Holt J W, Jacobel R W, Jenkins A, Jokat W, Jordan T, King E C, Kohler J, Krabill W, Riger-Kusk M, Langley K A, Leitchenkov G, Leuschen C, Luyendyk B P, Matsuoka K, Mouginot J, Nitsche F O, Nogi Y, Nost O A, Popov S V, Rignot E, Ripplin D M, Rivera A, Roberts J, Ross N, Siegert M J, Smith A M, Steinhage D, Studinger M, Sun B, Tinto B K, Welch B C, Wilson D, Young D A, Xiangbin C, Zirizzotti A. 2013. Bedmap2: improved ice bed, surface and thickness datasets for Antarctica, *The Cryosphere*, 7: 375-393
- Gkinis V, Popp T, Johnsen S, Blunier T. 2010. A continuous stream flash evaporator for the calibration of an IR cavity ring-down spectrometer for the isotopic analysis of water. *Isotopes in Environmental and Health Studies*.46:463–475.
- Gladstone R, Lee V, Rougier J, Payne A, Hellmer H, LeBrocq A, Shepherd A, Edwards T, Gregory J, Cornford S. 2012. Calibrated prediction of Pine Island Glacier retreat during the 21st and 22nd centuries with a coupled flow line model. *Earth and Planetary Science Letters*. 333-334: 191–199
- Goldstein R, Engelhardt H, Kamb B, Frolich R. 1993. Satellite Radar Interferometry for Monitoring Ice Sheet Motion: Application to an Antarctic Ice Stream. *Science*. 262: 1525-1530
- Gudmundsson H. 2006. Fortnightly variations in the flow velocity of Rutford Ice Stream, West Antarctica. *Nature*. 444: 1063-1064
- Gupta P, Noone D, Galewsky J, Sweeney C, Vaughn B. 2009. Demonstration of high-precision continuous measurements of water vapor isotopologues in laboratory and remote field deployments using wavelength-scanned cavity ring-down spectroscopy (WS-CRDS) technology. *Rapid Communications in Mass Spectrometry*. 23: 2534–2542
- Hallock A, Berman E, Zare R. 2002. Direct Monitoring of Absorption in Solution by Cavity Ring-Down Spectroscopy. *Analytical Chemistry*. 74: 1741-1743
- Hammer C, Clausen B, Langway C. 1997. 50,000 years of recorded global volcanism. *Climatic Change*. 35: 1-15
- Hanna E, Navarro F, Pattyn F, Domingues C, Fettweis X, Ivins E, Nicholls R, Ritz C, Smith B, Tulaczyk S, Whitehouse P, Zwally H. 2013. Ice-sheet mass balance and climate change. *Nature*. 498: 51-59
- Hindmarsh R, King E, Mulvaney R, Corr H, Hiess G, Gillet-Chaulet F. 2011. Flow at ice-divide triple junctions: 2. Three-dimensional views of isochrone architecture from ice-penetrating radar surveys. *Journal of Geophysical Research*. 116
- Hoshina Y, Fujita K, Nakazawa F, Iizuka Y, Miyake T, Hirabayashi M, Kuramoto T, Fujita S, Motoyama H. 2014. Effect of accumulation rate on water stable isotopes of near-surface snow in inland Antarctica. *Journal of Geophysical Research- Atmosphere*. 119, 274–283
- Hughes T. 1981. The weak underbelly of the West Antarctic ice-sheet. *Journal of Glaciology*. 27: 518–525
- Iizuka Y, Fujii Y, Hirasawa N, Suzuki T, Motoyama H, Furukawa T, Hondoh T. 2004. SO42- minimum in summer snow layer at Dome Fuji, Antarctica, and the probable mechanism. *Journal of Geophysical Research*. 109
- Isaksson E, Karlen W, Gundestrup N, Mayewski P, Whitlow S, Twickler M. 1996. A century of accumulation and temperature changes in Dronning Maud Land, Antarctica. *Journal of Geophysical Research*. 101: 7,085-7,094
- Ivask J, Pentchuk J, Vaikmäe J. 2001. Ion Chromatographic Determination of Major Anions and Cations in Antarctic Ice. *Proceedings of the Estonian Academy of Science- Chemistry*. 50: 46–51
- Ivask J, Pentchuk J, Vaikmae R. 2001. Ion chromatographic determination of major anions and cations in Antarctic ice. *Proceedings of the Estonian Academy of Sciences, Chemistry*. 50: 46–51

- Johnsen S, Clausen H, Cuffey K, Hoffmann G, Schwander J, Creyts T. 2000. Diffusion of stable isotopes in polar firn and ice: the isotope effect in firn diffusion. *Proceedings. Physics of Ice Core Records*. Pp285-305
- Johnson J, Bentley M, Smith A, Finkel C, Rood D, Gohl K, Balco G, Larter R, Schaefer J. 2014. Rapid thinning of Pine Island Glacier in the early holocene. *Science*. 343:999-1001
- Joughin I, Alley R. 2011. Stability of the West Antarctic ice sheet in a warming world, *Nature Geoscience*, 4: 506-513
- Kaczmarska M, Isaksson E, Karlöf L, Brandt O, Winther J, Van De Wal R, Van Den Broeke M, Johnsen S. 2006. Ice core melt features in relation to Antarctic coastal climate. *Antarctic Science*. 18: 271–278
- Kaspari S, Mayewski P, Dixon D, Sneed S, Handley M. 2005. Sources and Transport Pathways of Marine Aerosol Species into West Antarctica, *Annals of Glaciology*. 41:1-9
- Kaspari S, Mayewski P, Dixon D, Spikes V, Sneed S, Handley M, Hamilton G. 2004. Climate Variability in West Antarctica Derived from Annual Accumulation-Rate Records from ITASE Firn/Ice Cores. *Annals of Glaciology*. 39: 585-594
- Kaufmann P, Fundel F, Fischer H, Bigler M, Ruth U, Udisti R, Hansson M, de Angelis M, Barbante C, Wolff E, Hutterli M, Wagenbach D. 2010. Ammonium and non-sea salt sulfate in the EPICA ice cores as indicator of biological activity in the Southern Ocean. *Quaternary Science Reviews*. 29: 313–323
- Kendall C, Caldwell E. 1998. Chapter 2: Fundamentals of Isotope Geochemistry, in *Isotope Tracers in Catchment Hydrology*, C. Kendall and J. J. McDonnell (Eds.), Elsevier Science B.V., Amsterdam. pp. 51-86.
- Kreutz K, Mayewski P. 2002. 1994 Siple Dome Ice Core Major Ion Dataset. IGBP Pages/World Data Center for Paleoclimatology Data Contribution Series #2002-046. NOAA/NGDC Paleoclimatology Program. Boulder CO, USA
- Kreutz K, Mayewski P. 1999. Spatial variability of Antarctic surface snow glaciochemistry: implications for palaeoatmospheric circulation reconstructions. *Antarctic Science*. 11: 105-118
- Kreutz K, Mayewski P, Meeker L, Twickler M, Whitlow S. 2000. The effect of spatial and temporal accumulation rate variability in West Antarctica on soluble ion deposition. *Geophysical Research Letters*. 27. 2517-2520
- Küttel M, Steig E, Ding Q, Monaghan A, Battisti D. 2012. Seasonal climate information preserved in West Antarctic ice core water isotopes: relationships to temperature, large-scale circulation, and sea ice. *Climate Dynamics*. 39: 1841–1857
- Legrand M. 1997. Ice-core records of atmospheric sulphur. *Philosophical Transactions of the Royal Society*. 352: 241-250.
- Legrand M, Ducroz F, Wagenbach D, Mulvaney R, Hall J. 1998. Ammonium in coastal Antarctic aerosol and snow: Role of polar ocean and penguin emissions. *Journal of Geophysical Research*, 103: 11,043-11,056
- Legrand M, Mayewski P. 1997. Glaciochemistry of Polar Ice Cores: A Review. *Reviews of Geophysics*. 35: 219-243
- Legrand M, Saigne C. 1988. Formate, Acetate and Methanesulfonate Measurements in Antarctic Ice: Some Geochemical Implications. *Atmospheric Environment*. 22: 1011-1017
- Levin S. 1997. Analysis of Ions using HPLC: Ion Chromatography. http://www.forumsci.co.il/HPLC/ion_chrm.html (accessed 21/08/2014)
- Lorius C, Merlivat L, Jouzel J, Pourchet M. 1979. A 30,000 yr isotope climatic record from Antarctic ice. *Nature*. 280. 644-648..
- Marie-Louise Siggaard-Andersen a,b, Paolo Gabrielli c,d, Jørgen Peder Steffensen b, Trine Strømfeldt b, Carlo Barbante c, Claude Boutron d, Hubertus Fischer a, Heinz Miller, 2007, Soluble and insoluble lithium dust in the EPICA Dome C ice core—Implications for changes of the East Antarctic dust provenance during the recent glacial–interglacial transition, *Earth and Planetary Science Letters* 258 (2007) 32–43
- Marie-Louise SIGGAARD-ANDERSEN,1 JÖrgen Peder STEFFENSEN,2 Hubertus FISCHER1 2002 Lithium in Greenland ice cores measured by ion chromatography, *Annals of Glaciology* 35 2002, 243-249

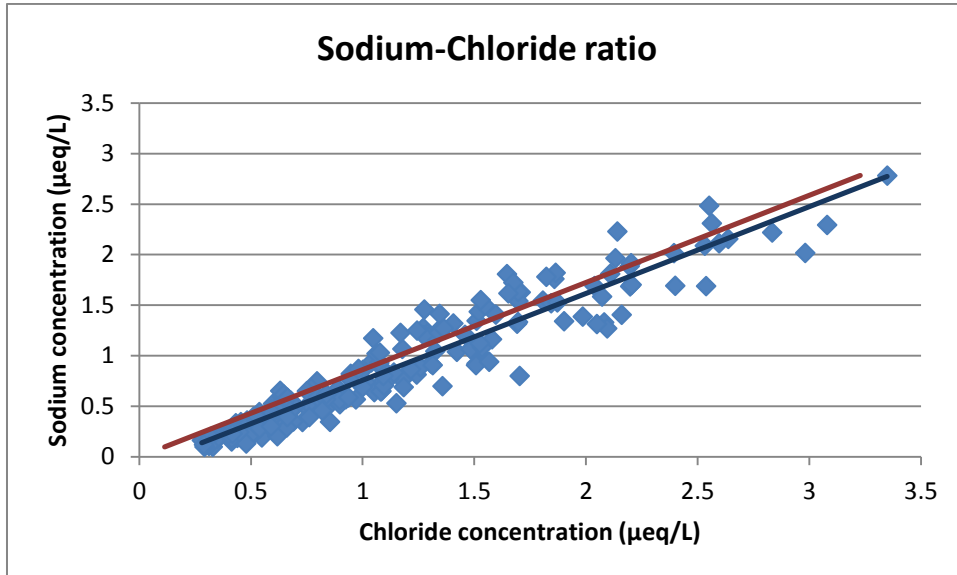
- Maselli O, Fritzsche D, Layman L, McConnell J Meyer H. 2013. Comparison of water isotope-ratio determinations using two cavity ringdown instruments and classical mass spectrometry in continuous ice-core analysis. *Isotopes in Environmental and Health Studies*. 49:387-398
- Medley B, Joughin I, Das S, Steig E, Conway H, Gogineni S, Criscitiello A, McConnell J, Smith B, van den Broeke M, Lenaerts J, Bromwich D, Nicola J. 2013. Airborne-radar and ice-core observations of annual snow accumulation over Thwaites Glacier, West Antarctica confirm the spatiotemporal variability of global and regional atmospheric models. *Geophysical Research Letters*. 40: 3649–3654
- Mercer J. 1978. West Antarctic ice sheet and CO₂ greenhouse effect: a threat of disaster. *Nature*. 271: 321-325
- Metrohm. 2014. Theory of Ion Chromatography, http://www.metrohm.co.uk/Downloads/Basic_Theories_IC.pdf (accessed 21/08/2014)
- Minikin A, Wagenbach D, Graf W, Kipfstuhl J. 1994. Spatial and seasonal variations of the snow chemistry at the central Filchner-Ronne Ice Shelf, Antarctica. *Annals of Glaciology*, 20: 238-290
- Mouginot J, Rignot E, Scheuchl B. 2014. Sustained increase in ice discharge from the Amundsen Sea Embayment, West Antarctica, from 1973 to 2013. *Geophysical Research Letters*. 41: 1576–1584
- Mulvaney R, Hall J, Wagenbach D, Legrand M, Ducroz F. 1998. Ammonium in coastal Antarctic aerosol and snow: Role of polar ocean and penguin emissions. *Journal of geophysical research*. 103: 11,043-11,056
- Mulvaney R, Wolff E. 1993. Evidence for winter/spring denitrification of the stratosphere in the nitrate record of Antarctic firn cores. *Journal of Geophysical Research*. 98: 5213–5220
- Mulvaney R, Wolff E. 1994. Spatial variability of the major chemistry of the Antarctic ice sheet. *Annals of Glaciology*. 20: 440-447
- NASA Earth Observatory (2011b) Paleoclimatology; the Oxygen balance, earthobservatory.nasa.gov/feaures/paleoclimatology_Oxygenbalance/, accessed 28/02/2011
- NSIDC: National Snow and Ice Data Centre. 2014a. Cryosphere Glossary. <http://nsidc.org/cryosphere/glossary-terms/snow>, accessed 29.08.2014
- NSIDC: National Snow and Ice Data Centre. 2014b. About Glaciers – what types of Glaciers are there? <http://nsidc.org/cryosphere/glaciers/questions/types.html> , accessed 29.08.2014
- NSIDC: National Snow and Ice Data Centre. 2014c. Cryosphere Glossary. <http://nsidc.org/cryosphere/glossary-terms/firn>, accessed 22.09.2014
- Olivier S, Schwikowski M, Brütsch S, Eyrikh S, Gäggeler H, Lüthi M, Papina T, Saurer M, Schotterer U, Tobler L, Vogel E. 2003. Glaciochemical investigation of an ice core from Belukha glacier, Siberian Altai. *Geophysical Research Letters*. 30: 2019-2022
- Park J, Gourmelen N, Shepherd A, Kim S, Vaughan D, Wingham D. 2013. Sustained retreat of the Pine Island Glacier. *Geophysical Research Letters*. 40: 2137–2142
- Pasteris D, McConnell J, Das S, Criscitiello A, Evans M, Maselli O, Sigl M, Layman L. 2014. Seasonally resolved ice core records from West Antarctica indicate a sea ice source of sea-salt aerosol and a biomass burning source of ammonium. *Journal of Geophysical Research - Atmosphere*. 119: 9168–9182
- Pfeiffer M, Dullo W, Eisenhauer A. 2004. Variability of the Intertropical Convergence Zone recorded in coral isotopic records from the central Indian Ocean (Chagos Archipelego). *Quaternary Research*. 61:245-255
- Picarro. 2014. Cavity Ring Down Spectroscopy. http://www.picarro.com/technology/cavity_ring_down_spectroscopy (accessed 25/08/2014)
- Rempel A. 2007. Formation of ice lenses and frost heave. *Journal of Geophysical Research*. 112
- Richardson C. 1976. Phase relationships in sea ice as a function of temperature. *Journal of Glaciology*. 17: 507-519
- Rignot E, Mouginot J, Morlighem M, Seroussi H, Scheuchl B. 2014. Widespread, rapid grounding line retreat of Pine Island, Thwaites, Smith, and Kohler glaciers, West Antarctica, from 1992 to 2011. *Geophysical Research Letters*. 41: 3502-3509

- Rippin D, Bingham R, Jordan T, Wright A, Ross N, Corr H, Ferraccioli F, Le Brocq A, Rose K, Siegert M. 2014. Basal roughness of the Institute and Möller Ice Streams, West Antarctica: Process determination and landscape interpretation. *Geomorphology*. 214: 139-144
- Traversi R, Udisti R, Frosini D, Becagli S, Ciardini V, Funke B, Lanconelli C, Petkov B, Scarchilli C, Severi M, Vitale V. 2014. Insights on nitrate sources at Dome C (East Antarctic Plateau) from multi-year aerosol and snow records. *Tellus B*. 66
- Ross N, Siegert M, Woodward J, Smith A, Corr H, Bentley M, Hindmarsh R, King E, Rivera A. 2011. Holocene stability of the Amundsen-Weddell ice divide, West Antarctica. *Geology*. 39:935-938
- Röthlisberger R, Abram N. 2009. Sea-ice proxies in Antarctic ice cores. *PAGES News* 17(1):24- 26.
- Runa Antony, Meloth Thamban, K P Krishnan and K Mahalinganathan, Is cloud seeding in coastal Antarctica Linked to bromine and nitrate variability In snow? *Environ. Res. Lett.* 5 (2010) 7pp
- Poluianov S, Traversi R, Usoskin I. 2014. Cosmogenic Production and climate contributions to nitrate record in the TALDICE Antarctic ice core. *Journal of Atmospheric and Solar-Terrestrial Physics*. 121: 50–58
- Scambos T, Bohlander J, Raup B, Haran T. 2004. Glaciological characteristics of the Institute Ice Stream using remote sensing. *Antarctic Science*. 16:205-213
- Schlosser E, Anshu H, Isaksson E, Martma T, Divine D, Nøst A. 2012. Surface mass balance and stable oxygen isotope ratios from shallow firn cores on Fimbulisen, East Antarctica. *Annals of Glaciology*. 53: 70-78
- Schwander J, Jouzel J, Hammer C, Petit J, Udisti R, Wolff E. 2001. A tentative chronology for the EPICA Dome Concordia ice core. *Geophysical Research Letters*. 28: 4243-4246
- Schwerzmann A, Funk M, Blatter H, Lüthi M, Schwikowski M, Palmer A. 2006. A method to reconstruct past accumulation rates in alpine firn regions: A study on Fiescherhorn, Swiss Alps. *Journal of Geophysical Research*. 111
- Schwikowski M, Eichler A. 2010. Alpine Glaciers as Archives of Atmospheric Deposition. In Bundi U. (ed.), *Alpine Waters, Handbook of Environmental Chemistry*. 6: 141-150.
- Schwikowski M, Schläppi M, Santibañez P, Rivera A, Casassa G. 2013. Net accumulation rates derived from ice core stable isotope records of Pío XI glacier, Southern Patagonia Icefield. *The Cryosphere*. 7: 1635–1644
- Siegert M, & Payne A. 2004. Past rates of accumulation in central West Antarctica. *Geophysical Research Letters*. 31
- Siegfried M, Fricker H, Roberts M, Scambos T, Tulaczyk S. 2014. A decade of West Antarctic subglacial lake interactions from combined ICESat and CryoSat-2 altimetry, *Geophysical Research Letters*, 41: 891-898
- Smith A. 1997. Basal conditions on Rufford Ice Stream, West Antarctica, from seismic observations. *Journal of Geophysical Research*, 102: 543-552
- Smithsonian Institute. 2013. Global Volcanism Program: Puyehue-Cordón Caulle. <http://www.volcano.si.edu/volcano.cfm?vn=357150> , Accessed 29/10/2014
- Sofen E, Alexander B, Steig E, Thiemens M, Kunasek S, Amos H, Schauer A, Hastings M, Bautista J, Jackson T, Vogel L, McConnell J, Pasteris D, Saltzman E. 2014. WAIS Divide ice core suggests sustained changes in the atmospheric formation pathways of sulfate and nitrate since the 19th century in the extratropical Southern Hemisphere. *Atmospheric Chemistry and Physics*. 14: 5749–5769
- Sommer S, Wagenbach D, Mulvaney R, Fischer H. 2000. Glacio-chemical study spanning the past 2 kyr on three ice cores from Dronning Maud Land, Antarctica: 2. Seasonally resolved chemical records. *Journal of Geophysical Research*. 105: 29423–29433,
- Spikes V, Hamilton G, Arcone S, Steven A, Kaspari S, Mayewski P. 2004. Variability in Accumulation Rates from GPR Profiling on the West Antarctic Plateau. *Earth Science Faculty Scholarship Paper* 208
- Stenni B, Serra F, Frezzotti M, Maggi V, Traverse R, Becagli S, Udisti R. 2000. Snow accumulation rates in northern Victoria Land, Antarctica, by firn-core analysis. *Journal of Glaciology*. 46: 541-552
- Suzuki K, Anzai K, Igarashi M, Motoyama H. 2005. High temporal resolution chemical analysis of H1, ice core in east Dronning Maud Land, Antarctica. *Polar Meteorology and Glaciology*. 19: 28-41

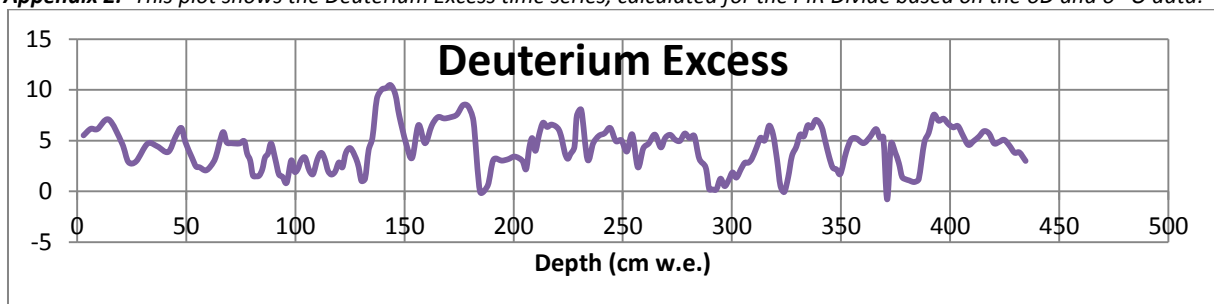
- Tedesco M, Monaghan A. 2009. An updated Antarctic melt record through 2009 and its linkages to high-latitude and tropical climate variability, *Geophysical Research Letters*. 36: L18502-L18506
- Thomas E, Dennis P, Bracegirdle T, Franzke C. 2009. Ice core evidence for significant 100-year regional warming on the Antarctic Peninsula. *Geophysical Research Letters*. 36
- Traversi R, Uditi R, Frosini D, Becagli S, Ciardini V, Funke B, Lanconelli C, Petkov B, Scarchilli C, Severi M, Vitale V. 2014. Insights on nitrate sources at Dome C (East Antarctic Plateau) from multi-year aerosol and snow records, *Tellus B*, 66
- Uditi R, Dayan U, Becagli S, Busetto M, Frosini D, Legrand M, Lucarelli F, Preunkert S, Severi M, Traversi R, Vitale V. 2012. Sea spray aerosol in central Antarctica. Present atmospheric behaviour and implications for paleoclimatic reconstructions. *Atmospheric Environment*. 52: 109-120
- UMM: University of Maine at Machias, Basic Principles of Ion Chromatography, <http://machias.edu/basic-principles-of-ion-chromatography.html> (accessed 19/08/2014)
- University of Copenhagen Centre for Snow and Ice (2014) Webpage: The firn zone: Transforming snow to ice, http://www.iceandclimate.nbi.ku.dk/research/drill_analysing/cutting_and_analysing_ice_cores/analysing_gasses/firn_zone/
- USGS: United States Geological Survey. 2014a. Geographic Names Information Systems. Pine Island Glacier. http://geonames.usgs.gov/apex/f?p=136:3:0::NO::P3_ANTAR_ID,P3_TITLE:11789,Pine%20Island%20Glacier
- USGS: United States Geological Survey. 2014b. Geographic Names Information Systems. Rutford Ice Stream. http://geonames.usgs.gov/apex/f?p=gnispq:5:0::NO::P5_ANTAR_ID:13077
- USGS: United States Geological Survey. 2014c. Geographic Names Information Systems. Institute Ice Stream. http://geonames.usgs.gov/apex/f?p=gnispq:5::NO::P5_ANTAR_ID:7326
- Vallelonga P, Gabrielli P, Rosman K, Barbante C, Boutron C. 2005. A 220 kyr record of Pb isotopes at Dome C Antarctica from analyses of the EPICA ice core. *Geophysical Research Letters*. 32
- Vaughan D. 2008. West Antarctic Ice Sheet collapse – the fall and rise of a paradigm. *Climatic Change*. 19: 65-79
- Welch B, Jacobel R. 2003. Analysis of deep-penetrating radar surveys of West Antarctica, US-ITASE 2001. *Geophysical Research Letters*. 30: 1444-1448
- Weller R, Wagenbach D, Legrand M, Elsässer C, Tian-Kunze X, König-Langlo G. 2011. Continuous 25-yr aerosol records at coastal Antarctica -I: inter-annual variability of ionic compounds and links to climate indices. *Tellus B*, 63: 901–919
- Whitlow S, Mayewski P, Dibb J. 1992. A Comparison of Major Chemical Species Seasonal Concentration and Accumulation at the South Pole and Summit, Greenland. *Atmospheric Environment*. 26A: 2045-2054
- Wilkens N, Behrens J, Kleiner T, Rippin D, Rückamp M, Humbert A. 2014. Thermal structure and basal sliding parametrisation at Pine Island Glacier– a 3-D full-Stokes model study. *The Cryosphere Discussions*. 8: 4913–4957
- Winstrup M, Vinther B, Sigl M, McConnell J, Svensson A, Wegner A. 2014. Development and comparison of layer-counted chronologies from the WAIS Divide and EDML ice cores, Antarctica, over the last glacial transition (10-15 ka BP). *Geophysical Research Abstracts*. 16
- Winther J, Bruland O, Sand K, Killingtveit Å, Marechal D. 1998. Snow accumulation distribution on Spitsbergen, Svalbard, in 1997. *Polar Research*. 17: 155-164
- Wolff E, Jones A, Bauguitte S, Salmon R. 2008. The interpretation of spikes and trends in concentration of nitrate in polar ice cores, based on evidence from snow and atmospheric measurements. *Atmospheric Chemistry and Physics*. 8: 5627-5634
- Xinqing L, Dahe Q, Jiawen R, Keqin D, Shichang K, Hui Z. 2002. Past 43 year oxalate record: Ürümqi glacier No.1, Tien Shan, China, and its link with Far East Rongbuk Glacier, Qomolangma (Mount Everest). *Annals of Glaciology*. 35: 285-290

11. Appendix

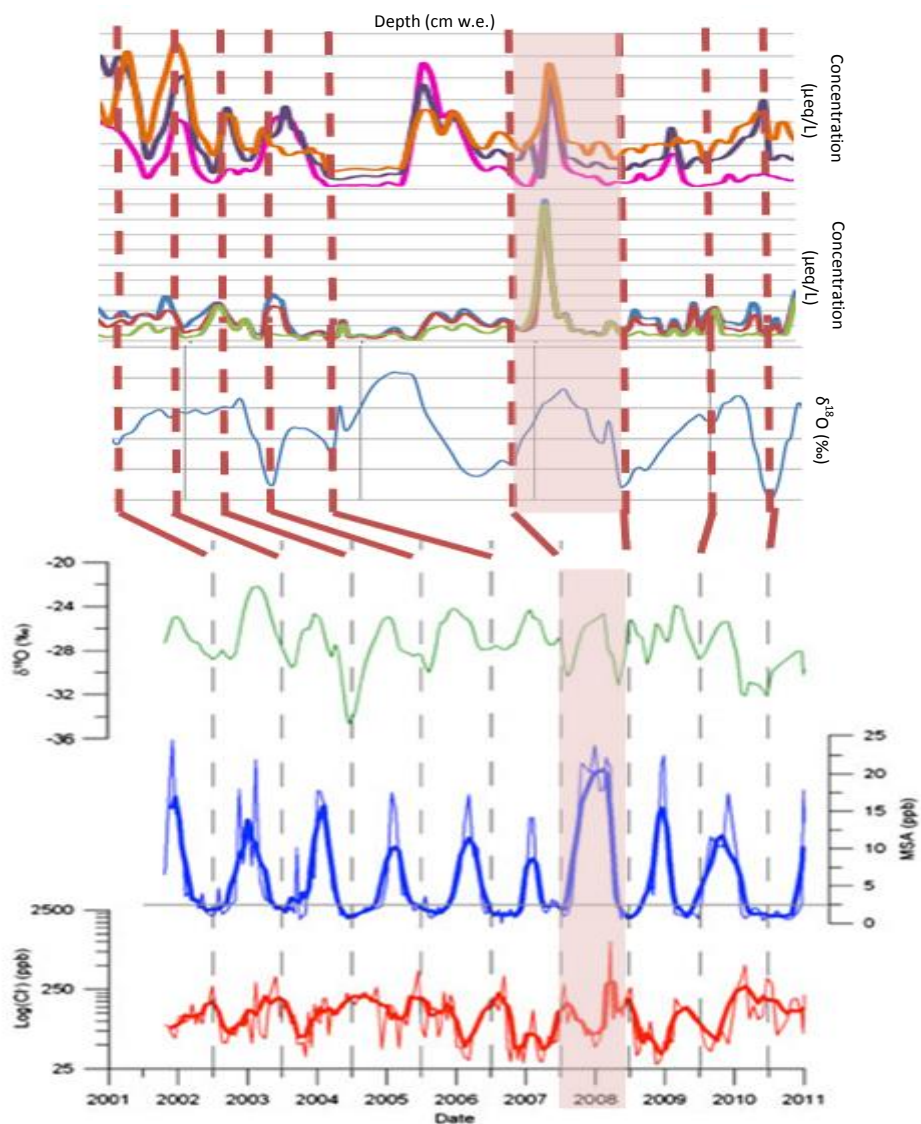
Appendix 1: This plot shows the ratio of sodium to chloride, as measured (blue dots, dark blue trendline) and in standard sea salt (red trendline) in sea water (Keene et al. 1986).



Appendix 2: This plot shows the Deuterium Excess time series, calculated for the PIR Divide based on the δD and $\delta^{18}O$ data.



Appendix 3: Plot comparing PIR divide ion and stable isotope data with data from another site in West Antarctica (Criscitiello et al. 2013). The top plot is PIR divide summer peaking ions; orange is NO_3^- , purple is nssSO_4^{2-} , pink is MSA. The second plot is PIR divide winter peaking ions; Green potassium, red sodium, blue chloride. The third plot is PIR divide $\delta^{18}\text{O}$. The lower three plots are labelled, and come from Criscitiello et al. (2013). The pink shading shows the year from winter 2007 to winter 2008 in both datasets. The timing of the anomalous peak, relative to summer 2007/08 is different.



Declaration

under Art. 28 Para. 2 RSL 05

Last, first name: FENWICK, JACQUELINE

Matriculation number: 13-127-949

Programme: Climate Sciences

Bachelor

Master

Dissertation

Thesis title: Determination of accumulation rates from a shallow firn core of the West Antarctic Ice Sheet

Thesis supervisor: Prof. Dr. Margit Schwikowski

I hereby declare that this submission is my own work and that, to the best of my knowledge and belief, it contains no material previously published or written by another person, except where due acknowledgement has been made in the text. In accordance with academic rules and ethical conduct, I have fully cited and referenced all material and results that are not original to this work. I am well aware of the fact that, on the basis of Article 36 Paragraph 1 Letter o of the University Law of 5 September 1996, the Senate is entitled to deny the title awarded on the basis of this work if proven otherwise.

.....
Place, date

.....
Signature